

ESI-Electronic Supplementary Material

Dendritic structured palladium complexes: Magnetically retrievable, highly efficient heterogeneous nanocatalyst for Suzuki and Heck cross-coupling reactions

Safoora Sheikh,^{a,b} Mohammad Ali Nasseri,^{*a} Mohammad Chahkandi,^{*c} Oliver Reiser^b and
Ali Allahresani^a

^aDepartment of Chemistry, Faculty of Basic Sciences, University of Birjand, P. O. Box 97175-615, Birjand, Iran

^bInstitut für Organische Chemie, Universität Regensburg, Universitätsstr. 31, 93053 Regensburg, Germany

^cDepartment of Chemistry, Faculty of Basic Sciences, Hakim Sabzevari University, P. O. Box 96179-76487, Sabzevar, Iran

*To whom correspondence should be addressed:

manaseri@birjand.ac.ir; Tel: +98-561-32202065 (M. A. Nasseri)

m.chahkandi@hsu.ac.ir; Tel.: +985144013342; Fax: +985144012451 (M. Chahkandi)

Table of Contents

1. Methods and Materials.....	S3
1.1 General.....	S3
1.2 Preparation of PAMAM dendrimer core with four ester groups.....	S4
1.3 Preparation of PAMAM dendrimer G ₀	S4
1.4 Synthesis of PAMAM G ₀ -Pd@ γ -Fe ₂ O ₃ MNPs.....	S5
1.5 General procedure for the Suzuki-Miyaura cross-coupling reaction.....	S6
1.6 General procedure for the Mizorki-Heck cross-coupling reaction.....	S7
2. Characterization of the PAMAM G ₀ -Pd@ γ -Fe ₂ O ₃ MNPs	S7
3. Screening of reaction conditions for the Suzuki-Miyaura reactions.....	S19
4. Screening of reaction conditions for the Mizorki-Heck reactions.....	S21
5. Experimental controls	S22
6. Recyclability Study	S22
7. Catalytic performance	S25
8. Data of Suzuki-Miyaura products.....	S26
9. Data of of Mizorki-Heck products.....	S34
10. References	S44

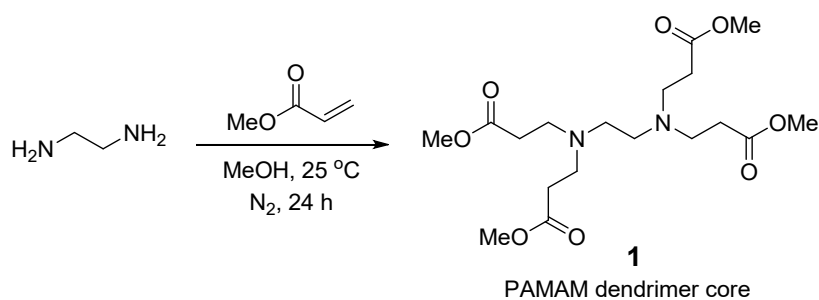
1. Methods and Materials

1.1 General

All starting materials were commercially available and used as received. Thin layer chromatography (TLC) was performed on silica-gel 60 F254 plates and UV light was used for visualization and also by GC-FID on a Shimadzu GC-16A instrument using a 25 m CBP1-S25 (0.32 mm ID, 0.5 μm coating) capillary column. Melting points were determined on a Tropical Labequip apparatus. The FT-IR spectra (JASCO-FT-IR 4600) were recorded using KBr pellet. The ^1H -NMR (300 and 250 MHz) and ^{13}C -NMR (75 and 62.9 MHz) spectra were recorded on a Bruker Avance DPX-300 spectrometer in the deuterated solvents (CDCl_3), using tetramethylsilane (TMS) as an internal standard. The Field emission scanning electron microscopy (FE-SEM) images of the prepared catalysts were taken on a Tescan MIRA3. EDX analysis were performed using a FESEM (JEOL-7600F-Oxford) equipped with a spectrometer of energy dispersion of X-ray. The presence of those elements was confirmed using the point elemental mapping (Tescan-Mira 3-SAMX). Liquid chromatography-mass spectrometry of PAMAM dendrimer G_0 was recorded by LC-Mass-AB SCIEX-Q-trap 3200 instrument. The microscopic images and size distribution of the catalyst NPs were performed using TEM (Philips-EM208) operating at 100 kV voltage. The X-ray diffraction (XRD) pattern were recorded by an X'pertpro (Philips) instrument employing $\text{Cu K}\alpha$ radiation ($\lambda = 1.5418 \text{ \AA}$), at a scanning speed of $2^\circ\text{C}/\text{min}$ from 10 to 80°C (2θ). TGA analysis of the samples were performed using a Q600 model from TA company made in U.S.A under nitrogen atmosphere with a heating rate of $15^\circ\text{C}/\text{min}$ in the temperature range of 25 – 800°C . The content of Pd in the catalyst was determined by OPTIMA 7300DV ICP analyzer. X-ray photoelectron spectroscopy (XPS) investigations were conducted on a XR3E2 (VG Microtech) twin anode X-ray source with $\text{Al-K}\alpha = 1486.6 \text{ eV}$. All the measured yields refer to the isolated products after purification

by the column chromatography. All the products characterized by NMR spectroscopy or GC. γ -Fe₂O₃ MNPs (**3**) were synthesized by a previously reported co-precipitation method.¹

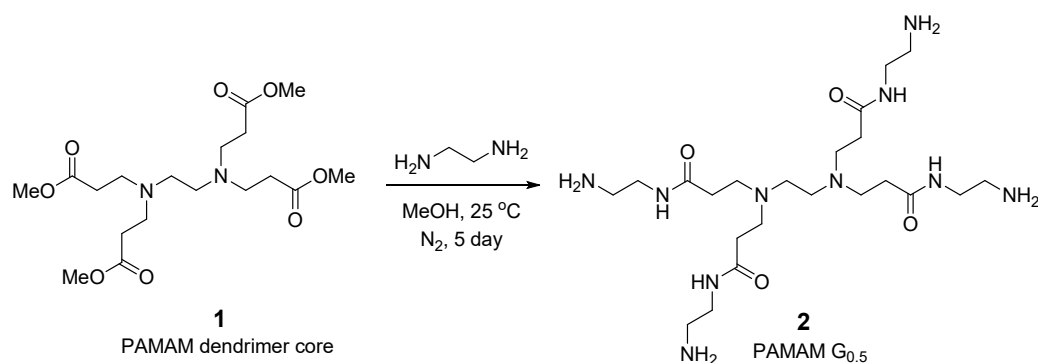
1.2. Preparation of PAMAM dendrimer core with four ester groups. PAMAM dendrimer core (**1**) was synthesized according to the previously reported method.² Briefly, methyl acrylate (14.3 g, 0.166 mol) was added dropwise to a methanolic solution (30 mL) of ethylenediamine (2.0 g, 33.3 mmol), during 50 min under nitrogen atmosphere at 0 °C. Then, the mixture was allowed to warm up to 25 °C and stirred during overnight. Subsequently, the mixture was concentrated under reduced pressure at 40 °C overnight, thus any excess reagent and solvent were removed. PAMAM dendrimer core with four ester groups, was obtained (13.5 g, 100% yield) and further used without purification (Scheme 1).



Scheme 1. Illustration of the preparation of the PAMAM dendrimer core.

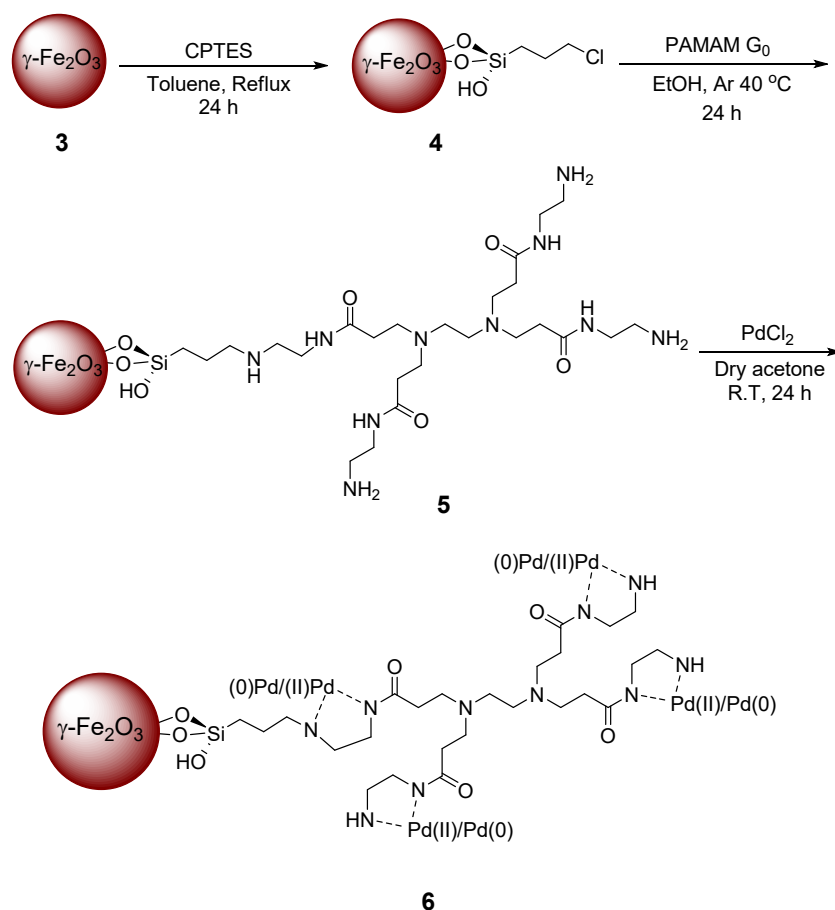
1.3. Preparation of PAMAM dendrimer G₀ (2**).** PAMAM dendrimer G₀ (**2**) was synthesized according to the previously reported method.² PAMAM dendrimer core (**1**) (2 g, 4.95 mmol) was dissolved in methanol (20 mL) and added dropwise into a methanolic solution of ethylenediamine (22.3 g, 0.371 mol in 50 mL) during 60 min. The reaction mixture was stirred under nitrogen atmosphere for 5 days at 25 °C. Then, the mixture was concentrated at reduced pressure for removing the excess content of ethylenediamine and solvent. In the end, traces of ethylenediamine was removed by dissolving the PAMAM dendrimer in 50 mL of butanol and this procedure was repeated to completion (ethylenediamine was detected by GCMS). The butanol was then removed under vacuum to yield PAMAM dendrimer G₀ (**2**) (3.05 g, about

96% yield) and obtained product having a very trace of butanol was further used without more purification (Scheme 2).



Scheme 2. Illustration of the preparation of the PAMAM dendrimer $G_{0.5}$.

1.4. Synthesis of PAMAM G_0 -Pd@ γ - Fe_2O_3 MNPs (6). First, γ - Fe_2O_3 (1.0 g) was suspended by sonication in dry toluene (30 mL) for 30 min. Then, (3-chloropropyl)triethoxysilane (0.963 g, 0.96 mL, 4.0 mmol) was added and the mixture was refluxed under nitrogen atmosphere for 24 h. After completion of the reaction, the solid product was separated from the solvent by an external magnet and washed twice with anhydrous toluene and diethyl ether and then dried under vacuum to yield γ - Fe_2O_3 @CPTES (**4**) (1.243 g).³ Afterwards PAMAM G_0 (3.416 g, 6.6 mmol, 4 mL) dissolved in ethanol (5 mL) was added dropwise to the dispersed Fe_2O_3 @CPTES (**4**) (1.0 g) in ethanol under Ar. Then the mixture was slowly stirred and heated at 40 °C for 24 h under Ar atmosphere. The product of PAMAM G_0 @ γ - Fe_2O_3 (**5**) was separated by an external magnet and washed with the ethanol followed by the vacuum drying at 40 °C, (1.310 g, 7.74% N determined by EDS). Finally, PAMAM G_0 @ γ - Fe_2O_3 (1.0 g) was added to a solution of palladium dichloride (0.136 g, 0.76 mmol) in dry acetone (20 mL). The reaction mixture was stirred at room temperature for 24 h. At the end, PAMAM G_0 -Pd@ γ - Fe_2O_3 (**6**) was separated by an external magnet, washed with acetone and ethanol, and dried in vacuum at 50 °C, at overnight (Scheme 3). ICP-OES results showed a loading of 0.073 g Pd / 1 gr of PAMAM G_0 -Pd@ γ - Fe_2O_3 (89%, 0.68 mmol of Pd).



Scheme 3. The synthesis of PAMAM G₀-Pd@γ-Fe₂O₃ (**6**).

1.5. General procedure for the Suzuki-Miyaura cross-coupling reaction (9a-r). Potassium carbonate (2.00 mmol) was added to a mixture of aryl halide (1.0 mmol) and phenylboronic acid (1.2 mmol) in water (2 mL), under stirring and heated at 60 °C (90 °C when we used aryl chlorides). Then PAMAM G₀-Pd@γ-Fe₂O₃ (**6**, 0.47 mol%, 0.007 g) was added to the resulting mixture under stirring. The progress of the reaction was monitored by TLC at different time intervals, until completion. Further the catalyst was separated by an external magnet and the reaction mixture was extracted with ethyl acetate (3 × 5 mL) (the residual solution along with the initial solution was used to identify and purify the product). Then, the combined organic phases were dried over anhydrous Na₂SO₄, and solvent evaporated. Eventually, all the products were characterized by GC or NMR spectroscopy (the crude coupling product was purified by using the silica-gel column chromatography, *n*-hexane/EtOAc, 8:2 eluent) (9a-r).

1.6. General procedure for the Mizoroki-Heck cross-coupling reaction (12a-r). PAMAM G_0 -Pd@ γ -Fe₂O₃ (6, 0.61 mol%, 0.009 g) was added to a mixture of K₂CO₃ (2.00 mmol), alkene (1.5 mmol), and aryl halide (1.0 mmol) in water (2 mL), under stirring and heated at 80 °C (90 °C when we used aryl chlorides) maintained in an oil bath. The reaction progress was screened by TLC at different time intervals. After the completion of the reaction, the nanocatalyst was separated by an external magnetic field. Then, remaining mixture was extracted with ethyl acetate (3 × 5 mL). The organic phase was completely dried over anhydrous Na₂SO₄, and solvent evaporated. Eventually, all the products were characterized by GC or NMR spectroscopy (the crude coupling product was purified by using the silica-gel column chromatography, *n*-hexane/EtOAc, 50:1 eluent) (12a-r).

2. Characterization of the PAMAM G_0 -Pd@ γ -Fe₂O₃ MNPs

The FT-IR spectra of PAMAM dendrimer core (1) and PAMAM dendrimer zero generation (G_0) (2) were recorded (Fig. S1). The peaks at 2935 and 2865 cm⁻¹ were attributed to the -CH₂ asymmetric and symmetric stretching modes, respectively. The observed peak at 1735 cm⁻¹ was matched with the stretching mode of C=O of PAMAM dendrimer core.⁴ As well as, peak at about 1000–1300 cm⁻¹ were related to the stretching vibration of C-N bond of PAMAM dendrimer core (Fig. S1a).⁵

The FT-IR spectrum of PAMAM G_0 showed major bands at about 3300–3500 cm⁻¹ which were attributed to the stretching mode of NH₂ groups (primary).⁶ The broad peak at 1650 cm⁻¹ was correspond to the stretching vibration of the amide groups -CONH- of PAMAM G_0 .⁷ The peaks at 2935 and 2865 cm⁻¹ were attributed to the asymmetric and symmetric -CH₂ stretching vibrations, respectively, and the peak about at 1559 cm⁻¹ can be assigned to the bending mode of NH₂ groups.⁸ Finally, the peak at about 1000-1300 cm⁻¹ was related to the C-N bond vibrations of PAMAM G_0 (Fig. S1b).⁵

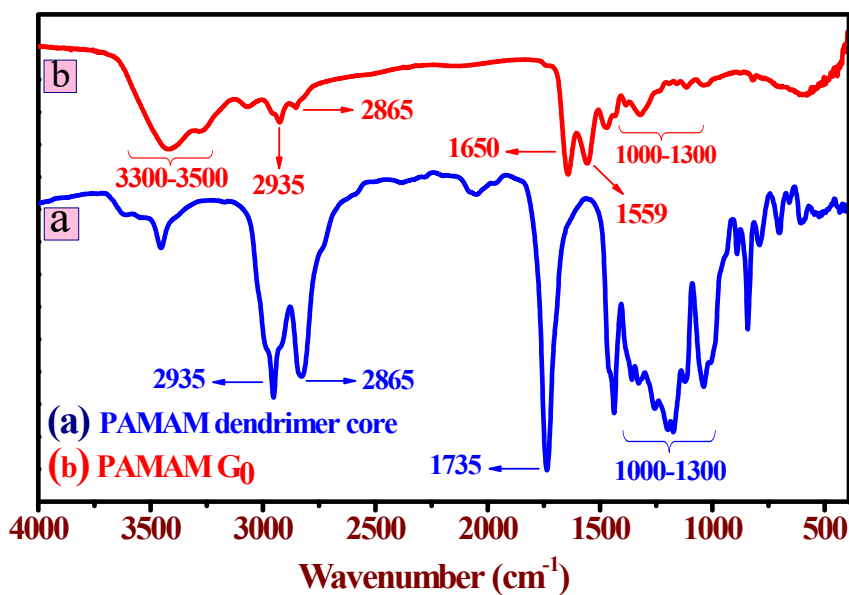


Fig. S1. FT-IR spectra of (a) PAMAM dendrimer core and (b) PAMAM dendrimer G₀.

The Figure S2 was depicted the FT-IR spectra of the consecutive synthetic parts of PAMAM G₀-Pd@ γ -Fe₂O₃ complex, as shown for γ -Fe₂O₃ (3), γ -Fe₂O₃@CPTES (4), γ -Fe₂O₃@PAMAM-G₀ (5), and PAMAM G₀-Pd@ γ -Fe₂O₃ complex (6). The strong absorption bond at 580 cm⁻¹ (Fig. 4a) was assigned to the stretching vibrations of Fe-O in γ -Fe₂O₃.^{9,10} Two absorption bands at 1075 and 1158 cm⁻¹ and a peak at 702 cm⁻¹ were attributed to the stretching vibrations of Si-O and C-Cl, respectively (Fig. S2b).^{11,12} The peaks positioned at 2935 and 2865, in the FT-IR spectra of γ -Fe₂O₃@CPTES and γ -Fe₂O₃@PAMAM-G₀ and PAMAM G₀-Pd@ γ -Fe₂O₃ were related to the stretching mode (asymmetric/symmetric), respectively (Fig. S2 b-d).^{13,14} Also, the peak at 1485 cm⁻¹ were related to the bending of the (-CH₂-) bonds (Fig. S2 b-d).^{13,14} The anchoring of PAMAM G₀ on γ -Fe₂O₃ was evidenced by the stretching mode of the carbonyl moiety of the amide group (-CONH-) appeared at 1650 cm⁻¹ (Fig. S2c).¹⁵ Also, the absorption bond recorded for γ -Fe₂O₃@PAMAM-G₀ at about 1543 cm⁻¹ was allocated to the bending mode of N-H.¹⁴ The known bands with medium intensity around of 3300-3500 cm⁻¹ regions are assigned to the N-H (primary) stretching vibration (Fig. S2c).¹⁵

Eventually, comparing of the FT-IR spectra of PAMAM dendrimer G₀ and PAMAM G₀-Pd@ γ -Fe₂O₃, showed the red shifting (~ 8 cm⁻¹) within the wavenumbers of stretching and bending modes of N-H (primary) that confirms the Pd metal coordination to the nitrogen atoms of PAMAM dendrimer G₀ (Fig. S2d). These results indicated that successful synthesis of the desired PAMAM G₀-Pd@ γ -Fe₂O₃ catalyst (see Fig. S2).

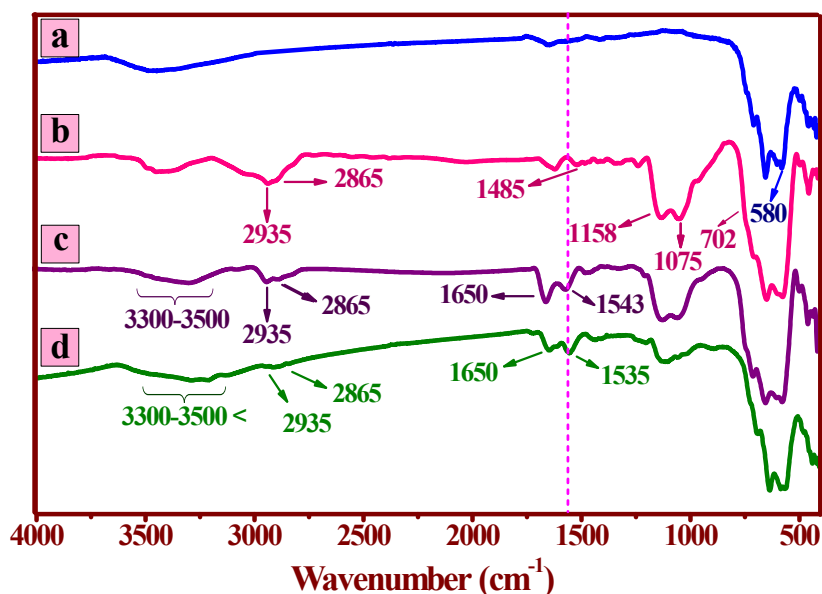


Fig. S2. FT-IR spectra of the (a) γ -Fe₂O₃, (b) γ -Fe₂O₃@CPTES, (c) γ -Fe₂O₃@PAMAM-G₀, (d) PAMAM G₀-Pd@ γ -Fe₂O₃.

The ¹H, ¹³C NMR spectra of PAMAM dendrimer core were recorded in CDCl₃ and TMS as a solvent and internal reference, respectively (Figures. S3-S6). NMR analysis of PAMAM dendrimer core (^aCH₂^aCH₂)[N(^bCH₂^cCH₂^dCO₂^eCH₃)₂]₂ gives useful information for structural specification. The ratio of protons, according to ¹H NMR spectrum information, from right to left in ¹H NMR image, is ^e12:^b8: ^a4:^c8 (Fig. S3). In the ¹H NMR spectrum, four H, related to (^aCH₂^aCH₂) groups of central core, was observed at δ 2.35 ppm (s, 4H). The presence of peaks at δ 2.62 and 2.29, appeared as two separate triplets (t, 8H), can be allocated to the two methylenes connected to the carbonyl group of ester (^bCH₂^cCH₂^dCO₂), respectively (Figures. S3 and S4). The resonance of hydrogens in methoxy groups (^dCO₂^eCH₃) was observed at δ 3.52 ppm (s, 12H) (Figures. S3 and S4). Also, the ¹³C NMR signals of

PAMAM dendrimer core ($^a\text{CH}_2^a\text{CH}_2$)[N($^b\text{CH}_2^c\text{CH}_2^d\text{CO}_2^e\text{CH}_3$) $_2$] $_2$ were appeared at c 32.47, b 49.64, a 51.29, e 52.11, d 172.71 (Figures. S5 and S6).

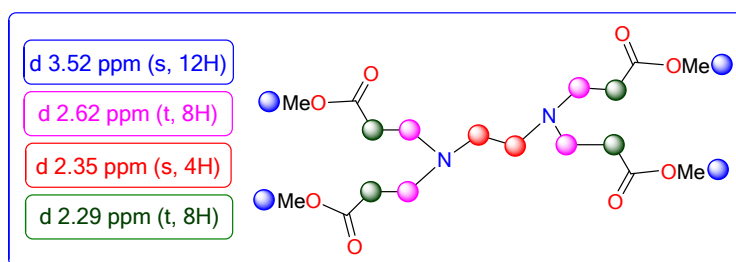


Fig. S3. $^1\text{H-NMR}$ chemical shifts of PAMAM dendrimer core (compound 1).

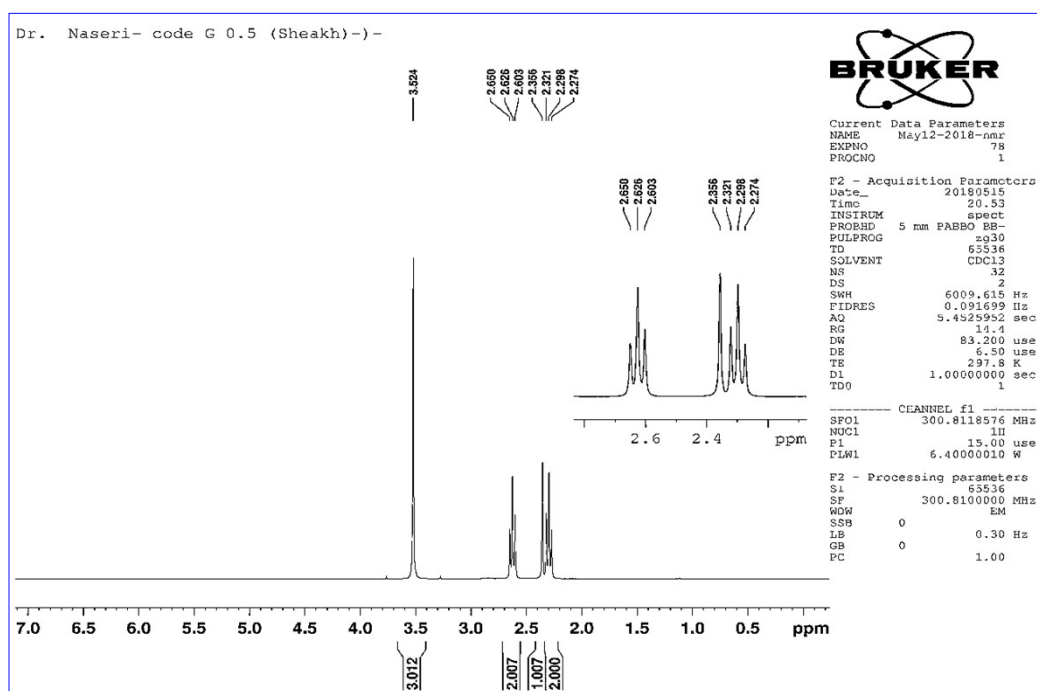


Fig. S4. $^1\text{H-NMR}$ (300 MHz, CDCl_3) spectrum of PAMAM dendrimer core (compound 1).

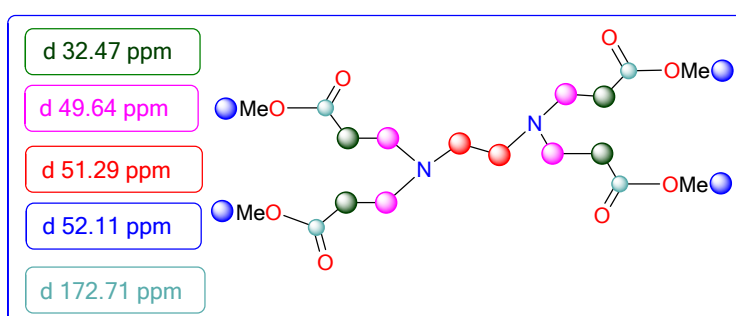


Fig. S5. $^{13}\text{C-NMR}$ chemical shifts of PAMAM dendrimer core (compound 2).

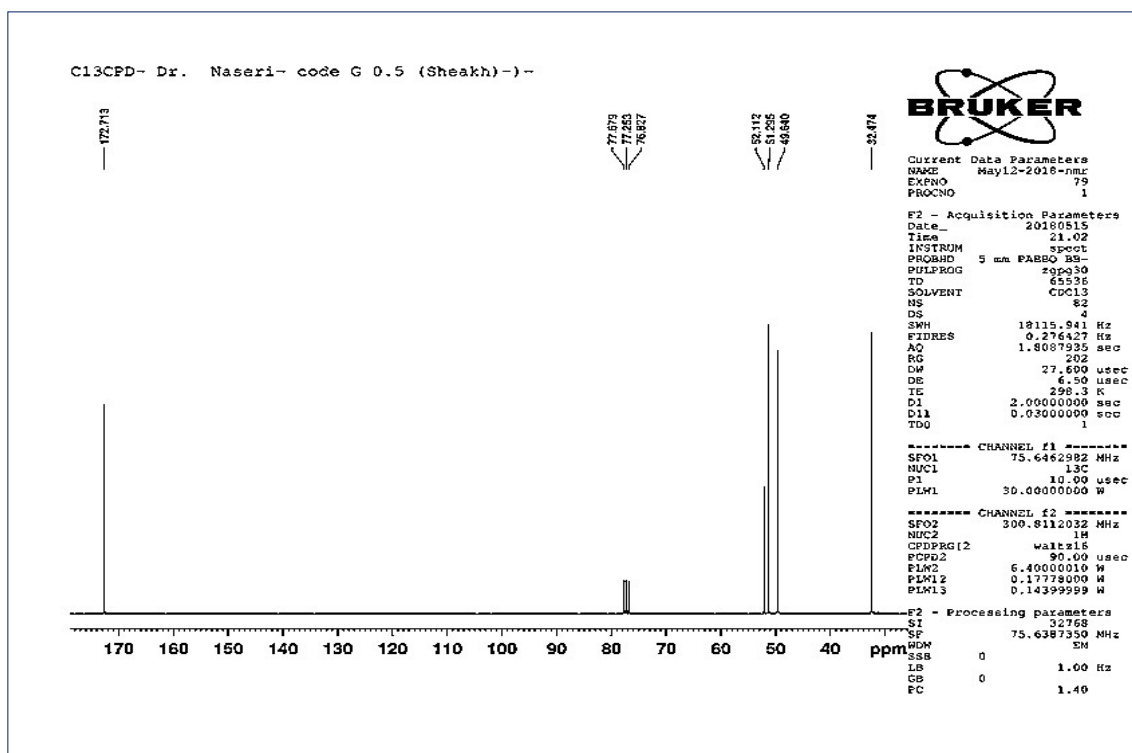


Fig. S6. ^{13}C -NMR (300 MHz, CDCl_3) spectrum of PAMAM dendrimer core (compound 2).

Printing Time: 12:48:45 PM
 Printing Date: February 17, 2020

Analyst Version: 1.6.3

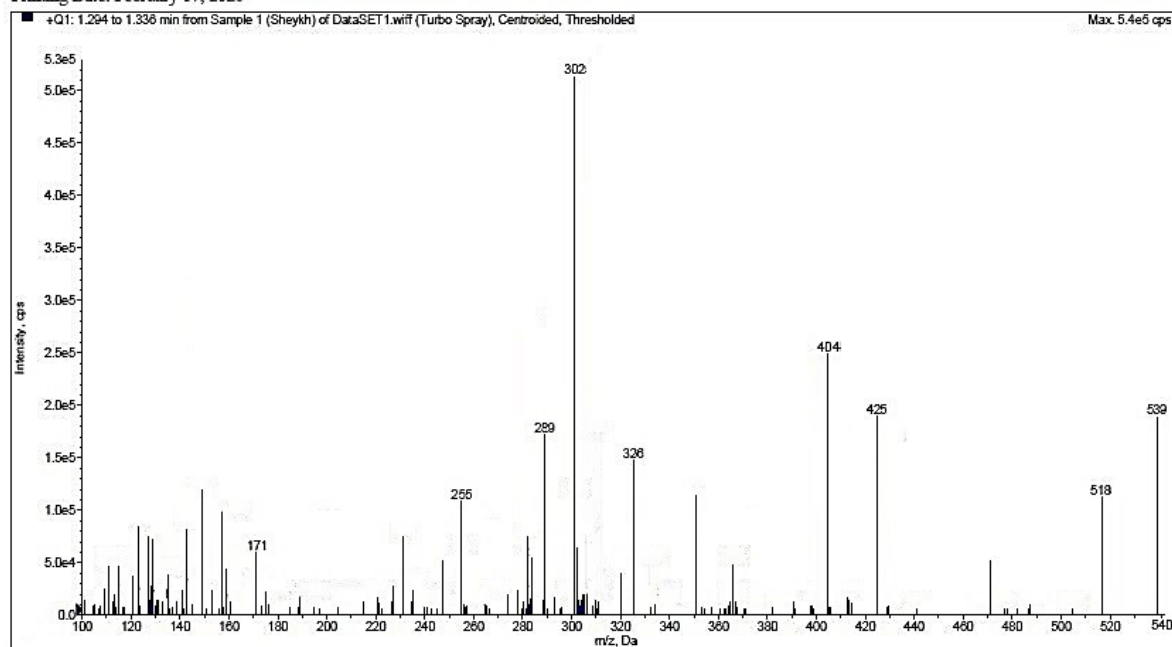


Fig. S7. LC-Mass spectra of (compound 2).

of the fragment structures of the ions corresponding to the PAMAM dendrimer G_0 , are listed in the ESI file (S6) (ESI, Figures. S7 and S8).

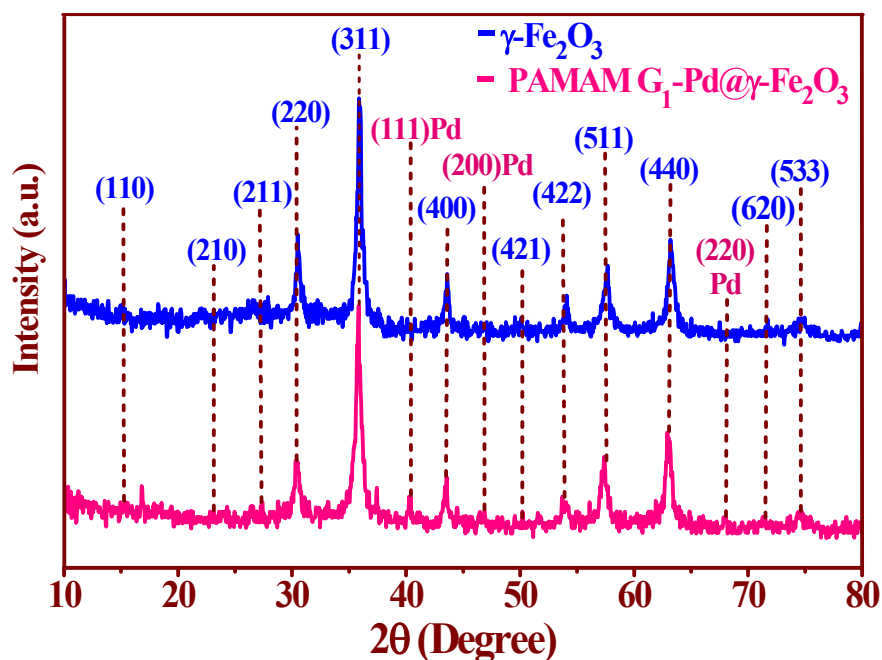


Fig. S9. XRD patterns of $\gamma\text{-Fe}_2\text{O}_3$, and PAMAM $G_0\text{-Pd}@ \gamma\text{-Fe}_2\text{O}_3$ complex.

The crystalline patterns of the purity $\gamma\text{-Fe}_2\text{O}_3$ MNPs and PAMAM $G_0\text{-Pd}@ \gamma\text{-Fe}_2\text{O}_3$ complex are presented in Figure S9. The XRD pattern of $\gamma\text{-Fe}_2\text{O}_3$ confirms the cubic magnetite crystal structure according to the appeared peaks at 15, 23.1, 26.9, 30.3, 35.8, 43.6, 50, 54.8, 57.3, 63.2, 71.1, and 74.4° (2θ), corresponded to the (110), (210), (211), (220), (311), (400), (421), (422), (511), (440), (620), and (533) miller indices, respectively (JCPDS card No. 39-1346)^{18,19} (see Fig. S9a). The observed diffraction peaks of PAMAM $G_0\text{-Pd}@ \gamma\text{-Fe}_2\text{O}_3$ at 40.1, 46.7 and 68.1° (2θ) are attributed to the standard crystallographic pattern of Pd NPs corresponded to the (111), (200), and (220) miller indices, (JCPDS Card No. 65-2867) (Fig. S9b).^{20,21} Decreasing of the XRD peaks intensity of PAMAM $G_0\text{-Pd}@ \gamma\text{-Fe}_2\text{O}_3$ catalyst can be related to the formation of palladium complexes on the surface of $\gamma\text{-Fe}_2\text{O}_3$ MNPs resulted in the stabilization of various functional groups including siloxy linkers and PAMAM dendrimer as ligands.

Besides, the average calculated crystalline size of PAMAM G_0 -Pd@ γ -Fe₂O₃ complex using Debye-Scherrer equation [$d=K\lambda/(\beta\cos\theta)$] is about 18.61 nm that shows good agreement from the direct method estimation of TEM images.

The FE-SEM images of γ -Fe₂O₃ NPs, γ -Fe₂O₃-CPTES and supported catalyst were shown in Figure S10. According to the FE-SEM image, the γ -Fe₂O₃ and γ -Fe₂O₃-CPTES NPs have a uniform spherical morphology (Fig. S10A). Also, the particles of the supported catalyst on the surface of γ -Fe₂O₃ NPs have a homogeneous spherical morphology and uniform size distribution. This clearly shows the synergistic effect of organic and inorganic diverse ingredients in a homogeneous network of PAMAM G_0 -Pd@ γ -Fe₂O₃ (**6**) (Fig. S10B).

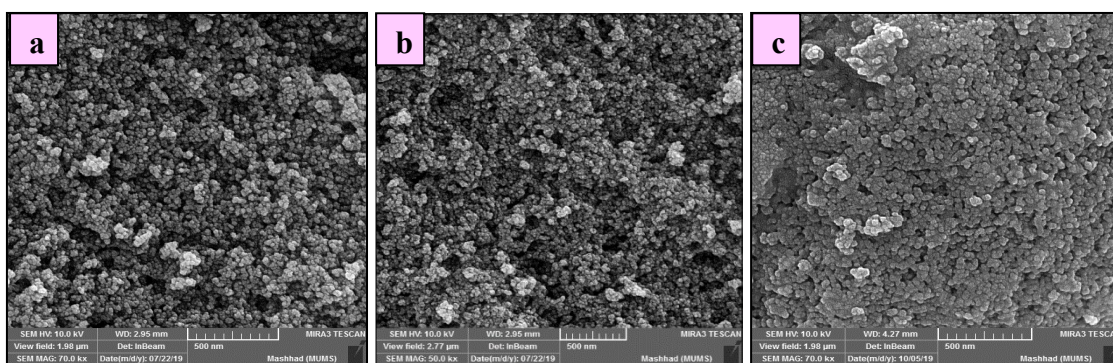


Fig. S10. FE-SEM images of the (a) γ -Fe₂O₃, (b) γ -Fe₂O₃-CPTES and (c) PAMAM G_0 -Pd@ γ -Fe₂O₃ complex.

The presence of elements in the catalyst were determined using energy-dispersive X-ray (EDX) study at random point on the surface of PAMAM G_0 -Pd@ γ -Fe₂O₃ (Fig. S11). The measurement results confirmed the presence of Pd, N, O, Si, Fe, Cl and C elements (8.10, 7.74, 21.03, 2.45, 43.79, 2.69 and 14.20 wt%, respectively) in the framework of PAMAM G_0 -Pd@ γ -Fe₂O₃ NPs (Fig. S11).

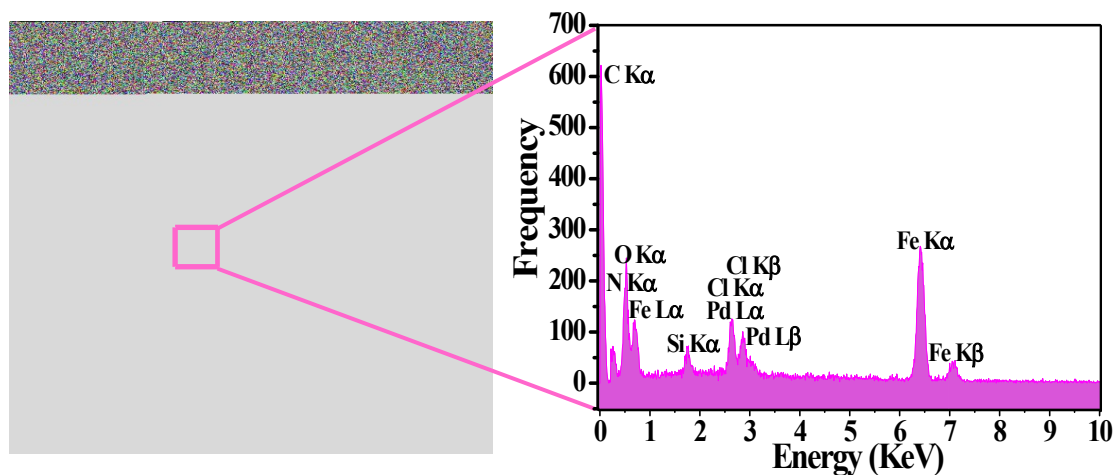


Fig. S11. EDX analysis of the PAMAM G_0 -Pd@ γ -Fe $_2$ O $_3$ complex.

The distribution of Pd NPs was studied by elemental mapping analysis of PAMAM G_0 -Pd@ γ -Fe $_2$ O $_3$ (Fig. S12). The EDS results clearly indicate that Pd NPs were dispersed almost uniformly and without aggregation on the catalyst surface (Fig. S12). Moreover, the presence of C, N, O, Si, Fe, and Pd elements was confirmed (Fig. S12).

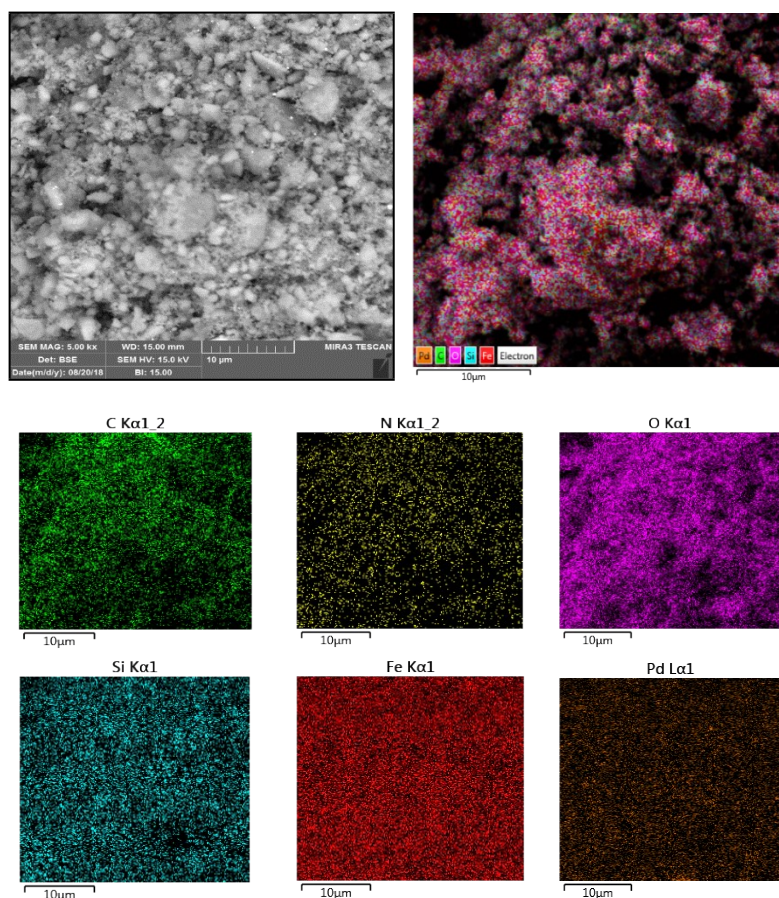


Fig. S12. EDS elemental mappings of the PAMAM G_0 -Pd@ γ -Fe $_2$ O $_3$ complex.

Also loading amount of the Pd on catalyst was determined. In order to find the loaded Pd content on the catalyst, it was digested with the concentrated HCl and HNO₃ and then was analyzed by ICP analysis. The measured values shown that 0.68 mmol of Pd was anchored on 1.0 g of PAMAM G₀-Pd@ γ -Fe₂O₃ complex.

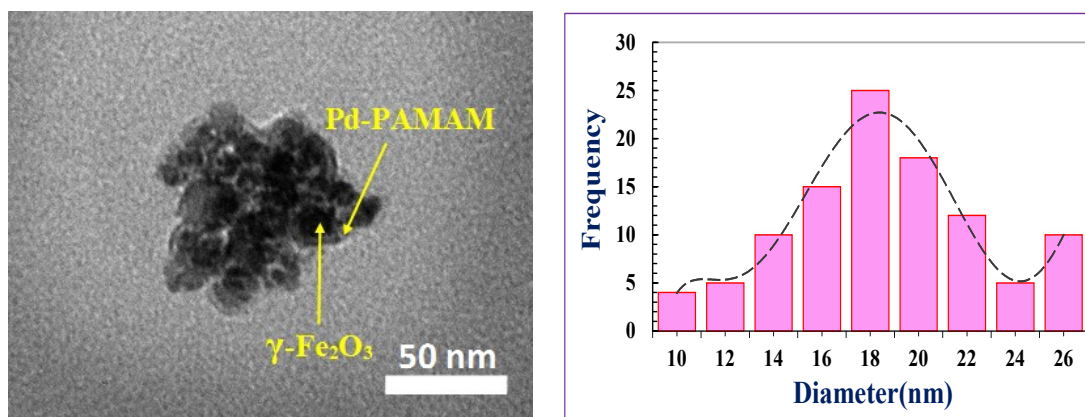


Fig. S13. (a) TEM images and (b) particles size distribution histogram of the PAMAM G₀-Pd@ γ -Fe₂O₃ complex.

The more detailed of morphology of PAMAM G₀-Pd@ γ -Fe₂O₃ was also investigated using TEM (Fig. S13A). The TEM image of catalyst clearly showed the uniform dispersion of nanosphere of PAMAM G₀-Pd@ γ -Fe₂O₃ as the core-organic shell structure of MNPs-Organic (Fig. S13A). It obviously indicates the average size of 18–20 nm for the Pd-complex (Fig. S13B).

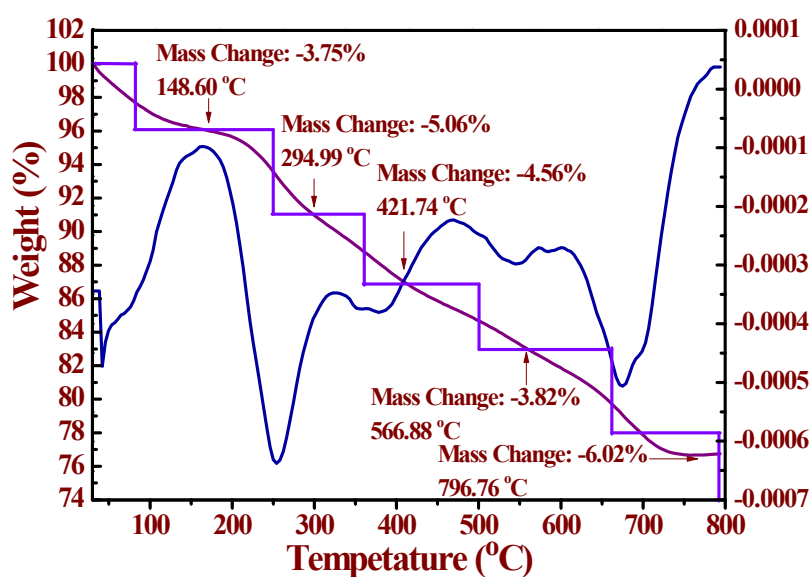


Fig. S14. TGA/DTG curve of the PAMAM G₀-Pd@ γ -Fe₂O₃ complex.

The TGA curves of $\gamma\text{-Fe}_2\text{O}_3$ MNPs and PAMAM $G_0\text{-Pd}@ \gamma\text{-Fe}_2\text{O}_3$ **6** were plotted at a heating rate of $15\text{ }^\circ\text{C min}^{-1}$ from $25\text{-}800\text{ }^\circ\text{C}$ under nitrogen atmosphere (Fig. S14). The curve of the PAMAM $G_0\text{-Pd}@ \gamma\text{-Fe}_2\text{O}_3$ complex exhibited five weight loss step in the temperature range of $25\text{-}800\text{ }^\circ\text{C}$ with a continuous weight loss. The initial weight loss up to $148.60\text{ }^\circ\text{C}$ was related to the loss of the adsorbed water molecules. The weight loss of 3.75%, 5.06, 4.56, and 3.82 in the second to fourth stages is due to the decomposition of the organic compounds and also the PAMAM dendrimer units grafted to the $\gamma\text{-Fe}_2\text{O}_3$ surface and removal of impurities in the prepared $\gamma\text{-Fe}_2\text{O}_3$, about 3.99% weight loss (Figures. S14 and S15 a, b). Actually, thermal treatment around of $300\text{-}570\text{ }^\circ\text{C}$ caused to the decomposition of organic sectors, fragmentation of structural components of PAMAM dendrimer, and breaking of siloxy linker bonds, included breaking of C-C, C-N, C-O, Si-C, Si-O, N-H and CH. Also, the weight lost in the fifth stage, near $800\text{ }^\circ\text{C}$ is attributed to the exhausting of the related oxygenated gases (CO_2 and so on) and N_2 (Fig. S14). In general, all of the data from TGA analysis, demonstrate the good thermal stability and only 23.21% weight loss of Pd-complex (Figures. S14 and S15 a, b).

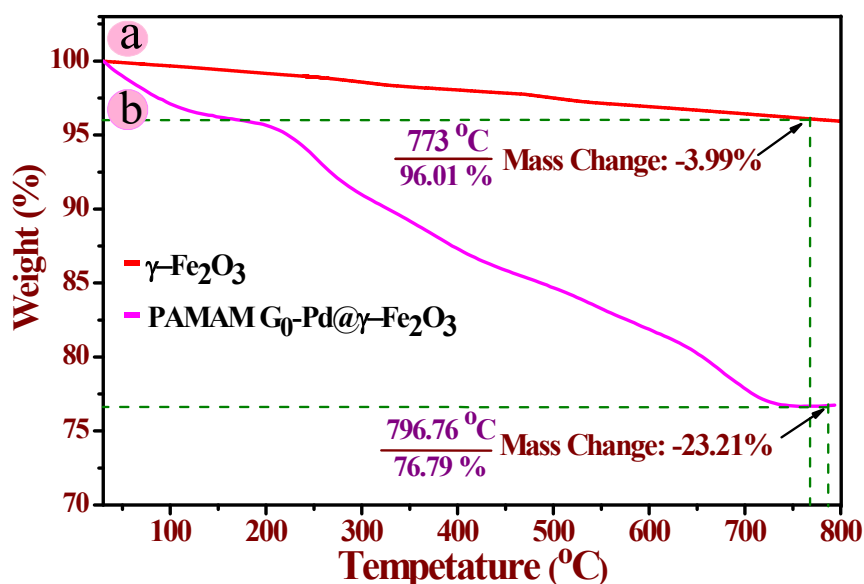


Fig. S15. TGA curves of the (a) $\gamma\text{-Fe}_2\text{O}_3$, and (b) PAMAM $G_0\text{-Pd}@ \gamma\text{-Fe}_2\text{O}_3$ complex.

The magnetic properties of the $\gamma\text{-Fe}_2\text{O}_3$ and PAMAM $\text{G}_0\text{-Pd}@ \gamma\text{-Fe}_2\text{O}_3$ were evaluated using the vibrating sample magnetometer (VSM) analysis at room temperature, which demonstrated the superparamagnetic characteristic of the $\gamma\text{-Fe}_2\text{O}_3$ and Pd-complex (cf. Figure S16 A). The measurements showed saturation magnetization values of 57.0, and 41.93 emu/g for $\gamma\text{-Fe}_2\text{O}_3$ and PAMAM $\text{G}_0\text{-Pd}@ \gamma\text{-Fe}_2\text{O}_3$ respectively (Figure S16A). The both compounds exhibited high permeability under magnetization, which was adequate to separate an external magnet field. Nevertheless, these results demonstrate that the magnetization of $\gamma\text{-Fe}_2\text{O}_3$ decreased considerably because of the fixation of siloxy linker and Pd-complex on the surface of $\gamma\text{-Fe}_2\text{O}_3$ (Figure 5). The magnetization curves did not display any of hysteresis phenomenon as the residue is equal to zero for both compounds (Figure. S16A). Moreover, the catalyst easily was separated using an external magnet from the aqueous solution (Figure S16 B).

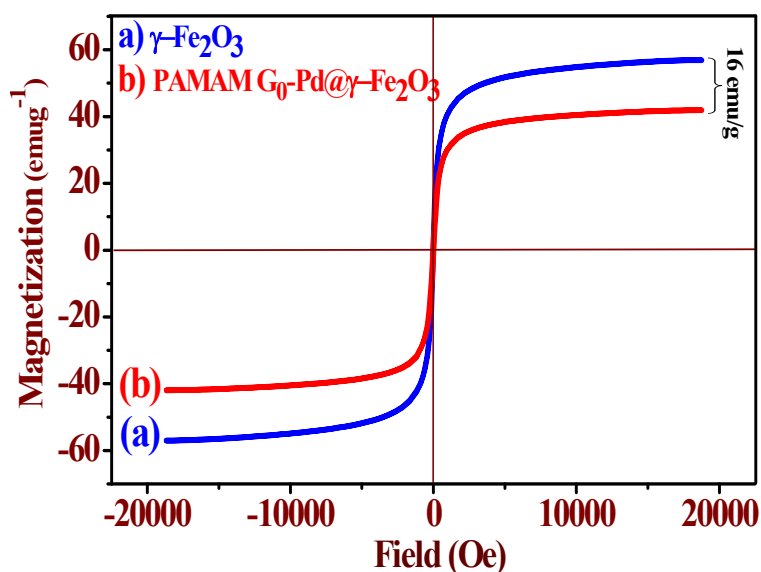


Fig. S16. Magnetization curves of (a) $\gamma\text{-Fe}_2\text{O}_3$, (b) PAMAM $\text{G}_0\text{-Pd}@ \gamma\text{-Fe}_2\text{O}_3$ at 300 K.

3. Screening of reaction conditions for the Suzuki-Miyaura reaction

The catalytic activity of PAMAM $\text{G}_0\text{-Pd}@ \gamma\text{-Fe}_2\text{O}_3$, within the Suzuki-Miyaura C-C coupling reaction was studied. The efficiency of this heterogeneous catalyst has been examined in the model cross-coupling reaction of iodobenzene with phenylboronic acid. The effect of solvent, temperature, amount of catalyst, and base type were appraised (Figure S18). The

optimum conditions of the mentioned ones can be regarded as water as solvent, K_2CO_3 as base, 60 °C at a catalyst loading of 0.47 mol%.

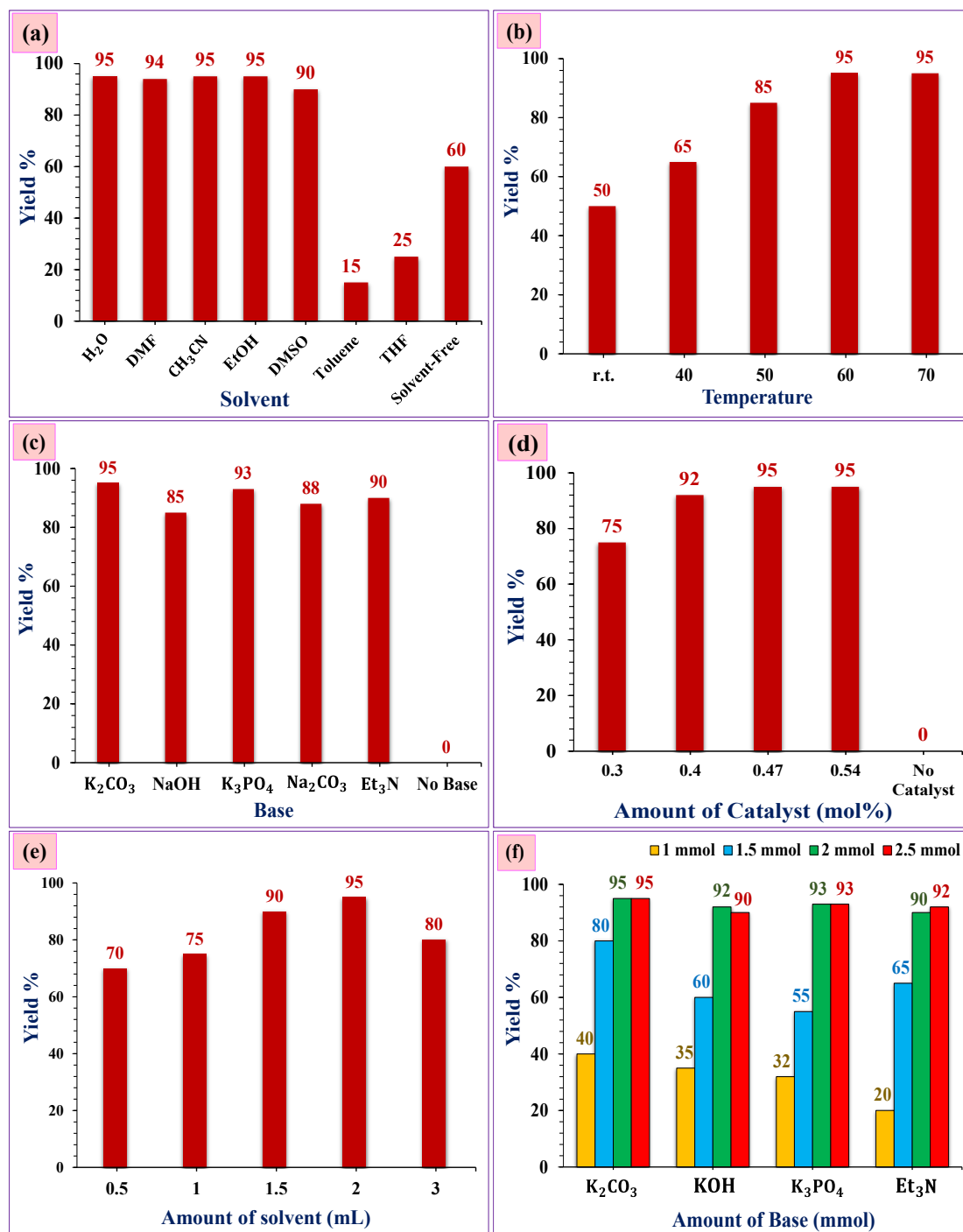


Fig. S17. Optimization of the reaction parameters for the Suzuki-Miyaura reaction: iodobenzene (1.0 mmol), phenylboronic acid (1.2 mmol), PAMAM G₀-Pd@ γ -Fe₂O₃ (0.47 mol% Pd, except (d)), 15 min, 60 °C (except (b)), K_2CO_3 (2 mmol, except (c)), H₂O (2 mL, except (a)); (a) Screening of different solvents (2 mL); (b) Screening of reaction temperature; (c) Screening of different bases (2 mmol); (d) Screening of catalyst amount; (e) Screening of solvent amount; (f) Screening of different amounts of bases (2 mmol).

4. Screening of reaction conditions for the Mizorki-Heck reactions

The catalytic activity of PAMAM G_0 -Pd@ γ -Fe $_2$ O $_3$, within the Mizorki-Heck C-C coupling reaction was studied. The efficiency of this heterogeneous catalyst has been examined in the model cross-coupling reaction of iodobenzene with styrene. The effect of solvent, temperature, amount of catalyst, and base type were appraised (Figure S18). The optimum conditions of the mentioned ones can be regarded as, water as solvent, K $_2$ CO $_3$ as base, 80 °C at a catalyst loading of 0.61 mol%.

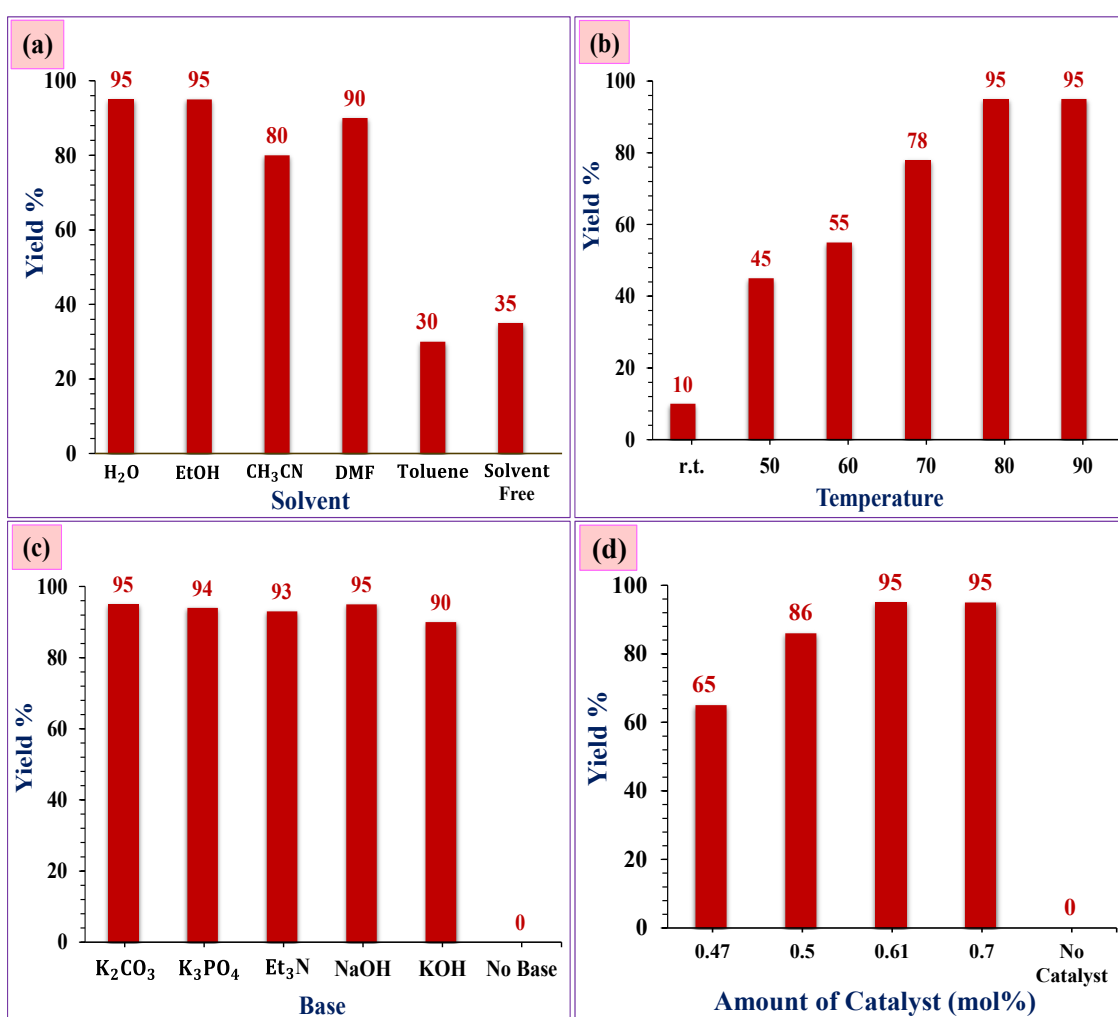


Fig. S18. Optimization of the reaction parameters on Mizorki-Heck reaction: iodobenzene (1.0 mmol) with styrene (1.5 mmol), catalyzed by PAMAM G_0 -Pd@ γ -Fe $_2$ O $_3$ (0.61 mol% Pd), for 60 min (except (d)); (a) Screening of different solvent (2 mL) using K $_2$ CO $_3$ (2 mmol), at 80 °C; (b) Screening of temperature, using K $_2$ CO $_3$ (2 mmol), H $_2$ O (2 mL); (c) Screening of different base (2 mmol), in H $_2$ O (2 mL), at 80 °C; (d) Screening of catalyst amount, using K $_2$ CO $_3$ (2 mmol), H $_2$ O (2 mL) catalyzed by Pd complex (0.61 mol% Pd) at 80 °C, after 60 min.

5. Experimental controls

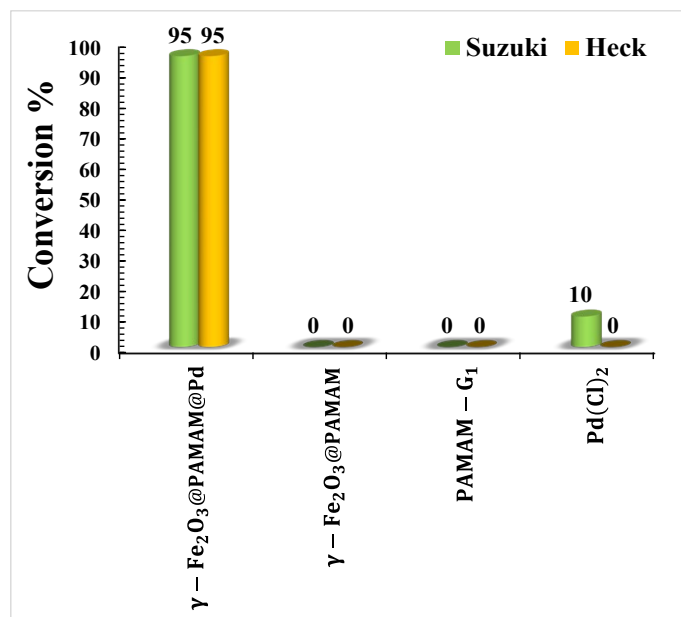


Fig. S19. Control experiments to show the catalytic activity of the PAMAM G₀-Pd@ γ -Fe₂O₃; Suzuki-Miyaura reaction: phenylboronic acid (1.2 mmol), iodobenzene (1.0 mmol), PAMAM G₀-Pd@ γ -Fe₂O₃ (0.47 mol % Pd), H₂O (2 mL), K₂CO₃ (2 mmol), 60 °C; Mizoroki-Heck reaction: styrene (1.5 mmol), iodobenzene (1.0 mmol), PAMAM G₀-Pd@ γ -Fe₂O₃ (0.61 mol % Pd), H₂O (2 mL), K₂CO₃ (2 mmol), 80 °C.

6. Recyclability Study for the Mizoroki-Heck reaction

A hot filtration test was performed to find out whether PAMAM G₀-Pd@-Fe₂O₃ acts as a heterogeneous catalyst. Toward this point, the model reaction of Heck-Mizoroki coupling was studied under the optimal conditions. In 28 min after starting of the coupling reaction between 4-iodobenzene and styrene, the catalyst was separated using an external magnetic and the reaction was then permitted to continue without catalyst for further 1 h. The reaction progress was followed by GC. There was no further coupling reaction, even after an extended time, indicated that a negligible amount of active species (less than 0.2% of Pd, according to the ICP-OES analysis) leaching out during the catalytic reaction. The results established the strong attachment of palladium nanoparticles to the PAMAM G₀-Pd@-Fe₂O₃ (see † Figure S20 for more details).

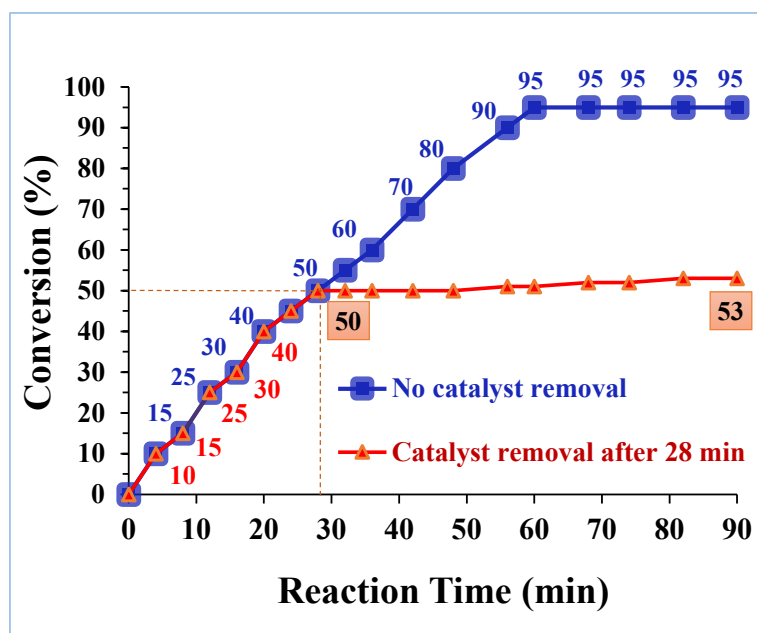


Fig. S20. Iodobenzene (1.0 mmol), styrene (1.5 mmol), PAMAM G_0 -Pd@ γ - Fe_2O_3 (0.47 mol % Pd), K_2CO_3 (2 mmol), 80 °C, in water (2 mL); Full conversion (blue squares) is reached after 60 min. In a second run (red triangles), the catalyst was removed by filtration after 28 min, upon which no further conversion was observed.

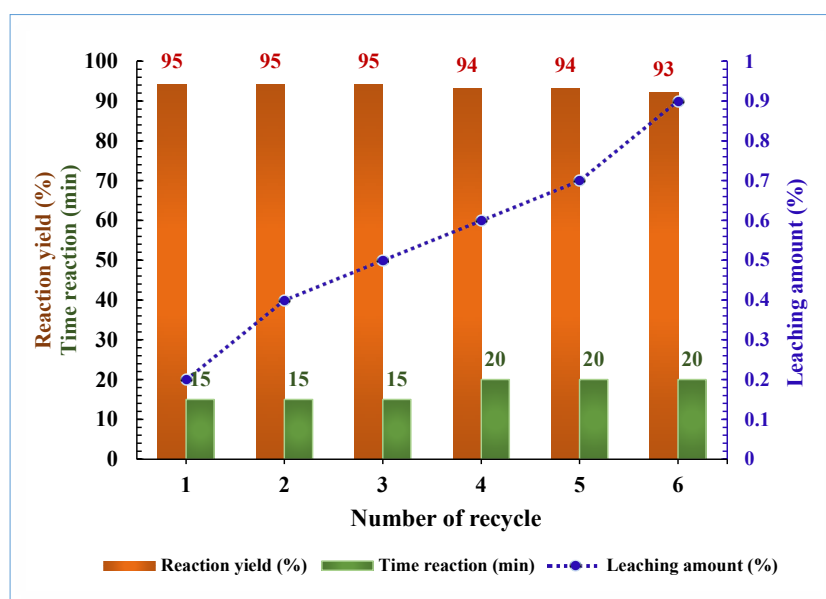


Fig. S21. Recycling and amount leaching of the catalyst during successive of Mizoroki–Heck cross–coupling reactions; Reaction conditions: styrene (1.5 mmol), iodobenzene (1.0 mmol), PAMAM G_0 -Pd@ γ - Fe_2O_3 (0.61 mol% Pd), H_2O (2 mL), K_2CO_3 (2 mmol), 80 °C, 60-80 min.

In order to quantitative analysis and realize the exact amount of palladium leaching for catalyst, after six consecutive runs, ICP-OES technique has been applied for the model reaction of Heck–Mizoroki coupling. The ICP-OES analysis showed, in totaly

less than 1% of palladium leaching after six serial runs of catalyst (see † Figure S21 for details).

Table 1. Recyclability of the catalyst in Suzuki-Miyaura and Mizorki-Heck reactions.

Reaction ^a	Run	Yield (%)	Time (min)	TON	TOF (h ⁻¹)
Suzuki-Miyaura	1	95	15	202	808
	2	95	15	202	808
	3	95	15	202	808
	4	95	15	202	808
	5	94	18	200	666
	6	93	20	197	596
Mizorki-Heck	1	95	60	155	155
	2	95	60	155	155
	3	95	60	155	155
	4	94	65	154	142
	5	94	70	154	132
	6	93	80	152	114

^aSuzuki-Miyaura reaction conditions: phenylboronic acid (1.2 mmol), iodobenzene (1.0 mmol), PAMAM G₀-Pd@ γ -Fe₂O₃ (0.47 mol %), H₂O (2 mL), K₂CO₃ (2 mmol), 60 °C, 15-20 min; Mizorki-Heck reaction conditions: styrene (1.5 mmol), iodobenzene (1.0 mmol), PAMAM G₀-Pd@ γ -Fe₂O₃ (0.61 mol% Pd), H₂O (2 mL), K₂CO₃, 80 °C, 60-80 min.

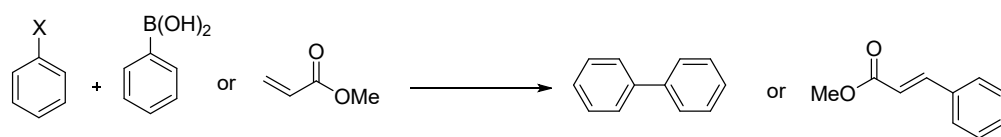
7. Catalytic performance

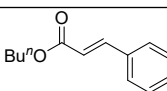
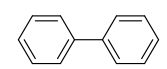
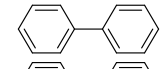
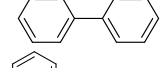
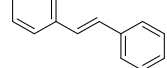
Table 2. Catalytic activity of the PAMAM G₀-Pd@ γ -Fe₂O₃ compared with some catalysts reported for Suzuki–Miyaura and Mizoroki–Heck.

Entry	Prod.	Catalyst (loading catalyst)	Conditions	Time (h)	Yield (%) ^a	Ref.
1		NHC ^b -Pd(II) complex (1.0 mol%)	THF ^c /Cs ₂ CO ₃ /80 °C	12	88	22
2		PdCl ₂ (0.05 mol%)	DMF ^d /Cs ₂ CO ₃ /130 °C	2	95	23
3		Pd/Au NPs (4.0 mol%)	EtOH-H ₂ O/K ₂ CO ₃ /80 °C	24	88	24
4		Pd-MPTAT ^e (0.02 gr)	DMF-H ₂ O/NaOH /85 °C	8	95	25
5	9d	Bis (oxamato) palladate (II) (5 mol%)	Bu ₄ NBr/Et ₃ N/120 °C	2	78	26
6		Pd-ZnFe ₂ O ₄ (4.62 mol%)	DMF/Et ₃ N/120 °C	4	92	27
7		Pd-Fe ₃ O ₄ (1 mol%)	DME ^f -H ₂ O/Na ₂ CO ₃ /Reflux	24	70	28
8		Pd@Mag-MSN ^g (1 mol%)	Dioxane/K ₂ CO ₃ /80 °C	6	77	29
9		Xerogel g ₁ -MNPs ^h (0.1 mol%)	MeOH/K ₂ CO ₃ /60 °C	5	89	30
10		bis(N-substituted)dioxamatopalladate (0.05 mmol)	DMF/Et ₃ N/80 °C	4	91	31
11		γ -Fe ₂ O ₃ @PAMAM-G ₀ -Pd (0.47 mol%)	H ₂ O/K ₂ CO ₃ /60 °C	0.25	95	This work
12		SiO ₂ @Fe ₃ O ₄ -Pd (0.5 mol%)	DMF/K ₂ CO ₃ /100 °C	8	97	32
13		HMMS ⁱ -NH ₂ -Pd (4 mol%)	NMP ^j /K ₂ CO ₃ /130 °C	8	98	33
14		TiO ₂ @Pd NPs (1.0 mol%)	DMF/Et ₃ N/140 °C	10	92	34
15	12j	Pd-Urea-MCF ^k (1 mol%)	Toluene/Et ₃ N/100 °C	20	92	35
16		Pd(0)-ZnFe ₂ O ₄ (4.62 mol%)	DMF/Et ₃ N/120 °C	3	90	27
17		Si-PNHC ^l -Pd (0.005 mmol)	NMP/K ₂ CO ₃ /120 °C	2	95	36
18		Pd-DABCO ^m - γ -Fe ₂ O ₃ (1-3 mol%)	Solvent-free/Et ₃ N/100 °C	0.5	92	1
19		γ -Fe ₂ O ₃ @PAMAM-G ₀ -Pd (0.61 mol%)	H ₂ O/K ₂ CO ₃ /80 °C	0.83	95	This work

^aIsolated yield; ^bNHC: N-heterocyclic Carbene; ^cTHF: Tetrahydrofuran; ^dDMF: Dimethylformamide; ^eMPTAT: N,N,N,N-tetramethylethylenediamine; ^fDME: Dimethoxyethane; ^gMSN: Mesoporous nanocomposite; ^hMNPs: Magnetic nanoparticles; ⁱHMMS: Hollow magnetic mesoporous spheres; ^jNMP: N-methyl-2-pyrrolidone; ^kSMF: Siliceous mesocellular foam; ^lPNHC: Polymeric N-heterocyclic carbene; ^m DABCO: 1,4-Diazabicyclo[2.2.2]octane.

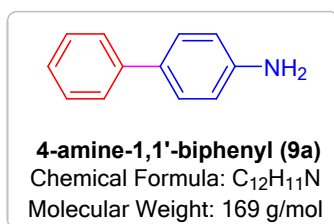
Table 3. Comparison leaching of some palladium hydrophilic/amphiphilic catalysts effective in c-c cross coupling reactions with PAMAM G₀-Pd@ γ -Fe₂O₃ catalyst.



Entry	Prod.	X	Cat.	Reaction conditions	Catalyst run	Pd leaching ^a	ref
1		I	Fe ₃ O ₄ @SiO ₂ @Im[Cl]Co ^(III) -melamine nanocomposite	EtOH/reflux	7 th	0.6	[37]
2		Br	Pd-NH ₂ -MPRN	K ₂ CO ₃ /H ₂ O: EtOH/80 °C	7 th	0.23	[38]
3		Br	Pd-NH ₂ -SBA-15	K ₂ CO ₃ /H ₂ O: EtOH/80 °C	7 th	0.79	[38]
4		I	MNPs@SiO ₂ @NH ₂ @Pd(dpa)Cl ₂	K ₂ CO ₃ /H ₂ O: EtOH/60 °C	15 th	1.01	[39]
5		I	PAMAM G ₀ -Pd@ γ -Fe ₂ O ₃	K ₂ CO ₃ /H ₂ O/60 °C	5 th	0.9	This work

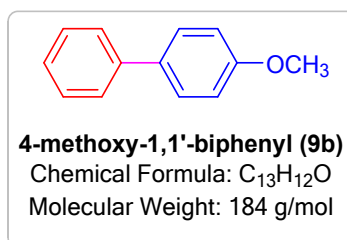
^aw/w% of Pd.

8. Data of Suzuki Products



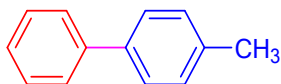
Phenylboronic acid (146.4 mg, 1.2 mmol) was reacted with 4-iodoaniline (219.0 mg, 1.00 mmol), K₂CO₃ (276.41 mg, 2.00 mmol) and γ -Fe₂O₃@PAMAM-G₀-Pd (7 mg, 0.47 mol%) in water at 60 °C to yield 85% (143.6 mg) 4-amine-1,1'-biphenyl (**9a**). Chromatography: n-hexane/EtOAc, 8:2. ¹H-NMR (CDCl₃, 250 MHz): δ 3.54 (s, 2H, NH₂), 6.66 (d, J = 4.75 Hz, 2H), 7.32-7.36 (m, 5H), 7.37 (m, 2H), 7.59 (d, J = 7.80 Hz, ArH).

Phenylboronic acid (146.4 mg, 1.2 mmol) was reacted with 4-chloroaniline (127.5 mg, 1.00 mmol), Et₃N (202.38 mg, 2.00 mmol) and γ -Fe₂O₃@PAMAM-G₀-Pd (7 mg, 0.47 mol%) in water at 90 °C to yield 65% (109.8 mg) 4-amine-1,1'-biphenyl (Product identification with GC, **9a**). Chromatography: n-hexane/EtOAc, 8:2.



Phenylboronic acid (146.4 mg, 1.2 mmol) was reacted with 1-iodo-4-methoxybenzene (234.0 mg, 1.00 mmol), K₂CO₃ (276.41 mg, 2.00 mmol) and γ -Fe₂O₃@PAMAM-G₀-Pd (7 mg, 0.47 mol%) in water at 60 °C to yield 92% (169.2 mg) 4-methoxy-1,1'-biphenyl (**9b**). Chromatography: n-hexane/EtOAc, 8:2. ¹H-NMR (CDCl₃, 300 MHz): δ 7.55-7.61 (m, 4H), 7.47 (d, J = 8.8 Hz, 2H), 7.30-7.37 (m, 1H), 7.03 (d, J = 8.8 Hz, 2H), 3.90 (s, 3H).

Phenylboronic acid (146.4 mg, 1.2 mmol) was reacted with 1-bromo-4-methoxybenzene (187.0 mg, 1.00 mmol), K₂CO₃ (276.41 mg, 2.00 mmol) and γ -Fe₂O₃@PAMAM-G₀-Pd (7 mg, 0.47 mol%) in water at 60 °C to yield 90% (165.6 mg) 4-methoxy-1,1'-biphenyl (Product identification with GC, **9b**).



4-methyl-1,1'-biphenyl (9c)

Chemical Formula: C₁₃H₁₂

Molecular Weight: 186 g/mol

Phenylboronic acid (146.4 mg, 1.2 mmol) was reacted with 1-iodo-4-methylbenzene (218.0 mg, 1.00 mmol), K₂CO₃ (276.41 mg, 2.00 mmol) and γ -Fe₂O₃@PAMAM-G₀-Pd (7 mg, 0.47 mol%) in water at 60 °C to yield 85% (158.0 mg) 4-methyl-1,1'-biphenyl (**9c**). Chromatography: n-hexane/EtOAc, 8:2. ¹H-NMR (CDCl₃, 300 MHz): δ 7.26-7.62 (m, 9H), 2.42 (s, 3H).

Phenylboronic acid (146.4 mg, 1.2 mmol) was reacted with 1-bromo-4-methylbenzene (171.0 mg, 1.00 mmol), K₂CO₃ (276.41 mg, 2.00 mmol) and γ -Fe₂O₃@PAMAM-G₀-Pd (7 mg, 0.47 mol%) in water at 60 °C to yield 75% (139.4 mg) 4-methyl-1,1'-biphenyl (**9c**). Chromatography: n-hexane/EtOAc, 8:2.

Phenylboronic acid (146.4 mg, 1.2 mmol) was reacted with 1-chloro-4-methylbenzene (126.5 mg, 1.00 mmol), Et₃N (202.38 mg, 2.00 mmol) and γ -Fe₂O₃@PAMAM-G₀-Pd (7 mg, 0.47 mol%) in water at 90 °C to yield 65% (120.9 mg) 4-methyl-1,1'-biphenyl (product identification with GC, **9c**). Chromatography: n-hexane/EtOAc, 8:2.



biphenyl (9d)

Chemical Formula: C₁₂H₁₀

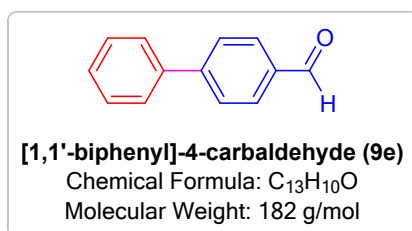
Molecular Weight: 154.21 g/mol

Phenylboronic acid (146.4 mg, 1.2 mmol) was reacted with iodobenzene (204.0 mg, 1.00 mmol), K₂CO₃ (276.41 mg, 2.00 mmol) and γ -Fe₂O₃@PAMAM-G₀-Pd (7 mg, 0.47 mol%) in water at 60 °C to yield 95% (146.4 mg) biphenyl (**9d**). Chromatography: n-hexane/EtOAc, 8:2. ¹H-NMR (CDCl₃, 300 MHz): δ 7.65-7.70 (m, 4H), 7.45-7.55 (m, 4H), 7.39-7.42 (m, 2H).

Phenylboronic acid (146.4 mg, 1.2 mmol) was reacted with bromobenzene (157.0 mg, 1.00 mmol), K₂CO₃ (276.41 mg, 2.00 mmol) and γ -Fe₂O₃@PAMAM-G₀-Pd (7 mg, 0.47 mol%) in water at 60 °C to

yield 95% (146.4 mg) biphenyl (product identification with GC, **9d**). Chromatography: n-hexane/EtOAc, 8:2.

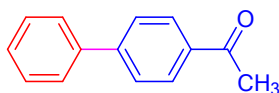
Phenylboronic acid (146.4 mg, 1.2 mmol) was reacted with chlorobenzene (112.5 mg, 1.00 mmol), Et₃N (202.38 mg, 2.00 mmol) and γ -Fe₂O₃@PAMAM-G₀-Pd (7 mg, 0.47 mol%) in water at 90 °C to yield 92% (141.8 mg) biphenyl (product identification with GC, **9d**). Chromatography: n-hexane/EtOAc, 8:2.



Phenylboronic acid (146.4 mg, 1.00 mmol) was reacted with 4-iodobenzaldehyde (232.0 mg, 1.00 mmol), K₂CO₃ (276.41 mg, 2.00 mmol) and γ -Fe₂O₃@PAMAM-G₀-Pd (7 mg, 0.47 mol%) in water at 60 °C to yield 93% (169.2 mg) [1,1'-biphenyl]-4-carbaldehyde (**9e**). Chromatography: n-hexane/EtOAc, 8:2. ¹H-NMR (CDCl₃, 300 MHz): δ 9.99 (s, 1H), 7.77 (d, J= 6.7, 2H), 7.70 (d, J= 6.7, 2H), 7.50-7.54 (m, 5H).

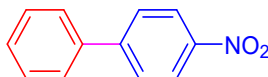
Phenylboronic acid (146.4 mg, 1.2 mmol) was reacted with 4-bromobenzaldehyde (185.0 mg, 1.00 mmol), K₂CO₃ (276.41 mg, 2.00 mmol) and γ -Fe₂O₃@PAMAM-G₀-Pd (7 mg, 0.47 mol%) in water at 60 °C to yield 85% (154.6 mg) [1,1'-biphenyl]-4-carbaldehyde (product identification with GC, **9e**). Chromatography: n-hexane/EtOAc, 8:2.

Phenylboronic acid (146.4 mg, 1.2 mmol) was reacted with 4-chlorobenzaldehyde (140.5 mg, 1.00 mmol), Et₃N (202.38 mg, 2.00 mmol) and γ -Fe₂O₃@PAMAM-G₀-Pd (7 mg, 0.47 mol%) in water at 90 °C to yield 75% (136.4 mg) [1,1'-biphenyl]-4-carbaldehyde (product identification with GC, **9e**). Chromatography: n-hexane/EtOAc, 8:2.



1-([1,1'-biphenyl]-4-yl)ethan-1-one (9f)
Chemical Formula: C₁₄H₁₂O
Molecular Weight: 196 g/mol

Phenylboronic acid (146.4 mg, 1.2 mmol) was reacted with 1-(4-bromophenyl)ethanone (199.0 mg, 1.00 mmol), K₂CO₃ (276.41 mg, 2.00 mmol) and γ -Fe₂O₃@PAMAM-G₀-Pd (7 mg, 0.47 mol%) in water at 60 °C to yield 95% (186.2 mg) [1,1'-biphenyl]-4-carbaldehyde (**9f**). Chromatography: n-hexane/EtOAc, 8:2. ¹H-NMR (CDCl₃, 300 MHz): δ 8.06 (d, J= 8.5 Hz, 2H), 7.70 (d, J= 8.5 Hz, 2H), 7.63-7.66 (m, 2H), 7.40-7.52 (m, 3H), 2.65 (s, 3H).

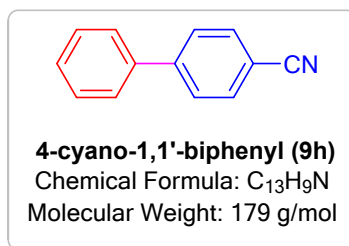


4-nitro-1,1'-biphenyl (9g)
Chemical Formula: C₁₂H₉NO₂
Molecular Weight: 199 g/mol

Phenylboronic acid (146.4 mg, 1.2 mmol) was reacted with 1-iodo-4-nitrobenzene (249.0 mg, 1.00 mmol), K₂CO₃ (276.41 mg, 2.00 mmol) and γ -Fe₂O₃@PAMAM-G₀-Pd (7 mg, 0.47 mol%) in water at 60 °C to yield 94% (187.0 mg) 4-nitro-1,1'-biphenyl (**9g**). Chromatography: n-hexane/EtOAc, 8:2. ¹H-NMR (CDCl₃, 300 MHz): δ 8.34 (d, J=6.9, 2H), 7.78 (d, J=6.9, 2H), 7.69 (d, J=7.9, 2H), 7.53 (d, J=7.9, 2H), 7.41-7.52 (m, 1H).

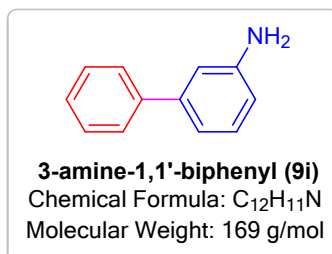
Phenylboronic acid (146.4 mg, 1.2 mmol) was reacted with 1-bromo-4-nitrobenzene (202.0 mg, 1.00 mmol), K₂CO₃ (276.41 mg, 2.00 mmol) and γ -Fe₂O₃@PAMAM-G₀-Pd (7 mg, 0.47 mol%) in water at 60 °C to yield 90% (179.0 mg) 4-nitro-1,1'-biphenyl (product identification with GC, **9g**). Chromatography: n-hexane/EtOAc, 8:2.

Phenylboronic acid (146.4 mg, 1.2 mmol) was reacted with 1-chloro-4-nitrobenzene (157.5 mg, 1.00 mmol), Et₃N (202.38 mg, 2.00 mmol) and γ -Fe₂O₃@PAMAM-G₀-Pd (7 mg, 0.47 mol%) in water at 90 °C to yield 87% (173.0 mg) 4-nitro-1,1'-biphenyl (product identification with GC, **9g**). Chromatography: n-hexane/EtOAc, 8:2.



Phenylboronic acid (146.4 mg, 1.2 mmol) was reacted with 4-bromobenzonitrile (182.0 mg, 1.00 mmol), K₂CO₃ (276.41 mg, 2.00 mmol) and γ -Fe₂O₃@PAMAM-G₀-Pd (7 mg, 0.47 mol%) in water at 60 °C to yield 80% (143.2 mg) 4-cyano-1,1'-biphenyl (**9h**). Chromatography: n-hexane/EtOAc, 8:2. ¹H-NMR (CDCl₃, 250 MHz): δ 7.41-7.48 (m, 3H), 7.58-7.76 (m, 6H).

Phenylboronic acid (146.4 mg, 1.2 mmol) was reacted with 4-chlorobenzonitrile (114.6 mg, 1.00 mmol), Et₃N (202.38 mg, 2.00 mmol) and γ -Fe₂O₃@PAMAM-G₀-Pd (7 mg, 0.47 mol%) in water at 90 °C to yield 70% (137.4 mg) 4-cyano-1,1'-biphenyl (product identification with GC, **9h**). Chromatography: n-hexane/EtOAc, 8:2.



Phenylboronic acid (146.4 mg, 1.2 mmol) was reacted with 3-iodoaniline (219.0 mg, 1.00 mmol), K₂CO₃ (276.41 mg, 2.00 mmol) and γ -Fe₂O₃@PAMAM-G₀-Pd (7 mg, 0.47 mol%) in water at 60 °C to yield 75% (126.6 mg) 3-amine-1,1'-biphenyl (**9i**). Chromatography: n-hexane/EtOAc, 8:2. ¹H-NMR (CDCl₃, 300 MHz): δ 7.24-7.32 (m, 3H), 6.85-6.9 (m, 3H), 6.73-6.79 (m, 3H), 3.65 (s, 2H, NH₂).

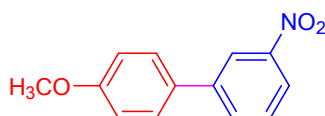


3-(trifluoromethyl)-1,1'-biphenyl (9j)

Chemical Formula: $C_{13}H_9F_3$

Molecular Weight: 184 g/mol

Phenylboronic acid (146.4 mg, 1.2 mmol) was reacted with 1-bromo-3-(trifluoromethyl)benzene (225.0 mg, 1.00 mmol), K_2CO_3 (276.41 mg, 2.00 mmol) and $\gamma-Fe_2O_3@PAMAM-G_0-Pd$ (7 mg, 0.47 mol%) in water at 60 °C to yield 90% (165.6 mg) 3-(trifluoromethyl)-1,1'-biphenyl (**9j**). Chromatography: n-hexane/EtOAc, 8:2. 1H -NMR ($CDCl_3$, 300 MHz): δ 7.80-7.90 (m, 4H), 7.64-7.66 (m, 2H), 7.25-7.30 (m, 3H).



4'-methyl-3-nitro-1,1'-biphenyl (9k)

Chemical Formula: $C_{13}H_{11}NO_3$

Molecular Weight: 229 g/mol

(4-methoxyphenyl)boronic acid (181.2 mg, 1.2 mmol) was reacted with 1-bromo-3-nitrobenzene (202.0 mg, 1.00 mmol), K_2CO_3 (276.41 mg, 2.00 mmol) and $\gamma-Fe_2O_3@PAMAM-G_0-Pd$ (7 mg, 0.47 mol%) in water at 60 °C to yield 90% (206.0 mg) 4'-methyl-3-nitro-1,1'-biphenyl (**9k**). Chromatography: n-hexane/EtOAc, 8:2. 1H -NMR ($CDCl_3$, 300 MHz): δ 8.45-8.47 (m, 1H), 8.18-8.21 (m, 1H), 7.91-7.94 (m, 1H), 7.62-7.65 (m, 1H), 7.62 (d, $J=8.5$ Hz, 2H), 7.07 (d, 2H), 3.92 (s, 3H).



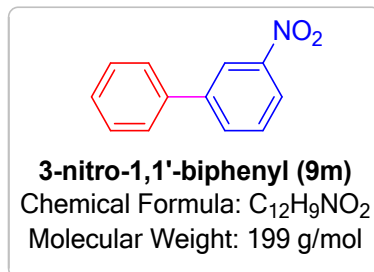
4'-methyl-3-nitro-1,1'-biphenyl (9l)

Chemical Formula: $C_{13}H_{11}NO_2$

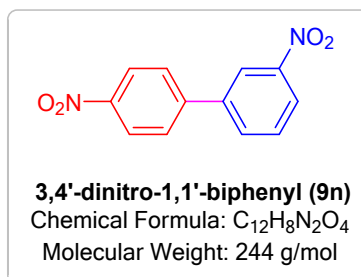
Molecular Weight: 213 g/mol

p-tolylboronic acid (162.0 mg, 1.2 mmol) was reacted with 1-bromo-3-nitrobenzene (202.0 mg, 1.00 mmol), K_2CO_3 (276.41 mg, 2.00 mmol) and $\gamma-Fe_2O_3@PAMAM-G_0-Pd$ (7 mg, 0.47 mol%) in water at

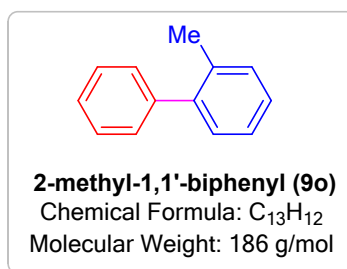
60 °C to yield 92% (195.8 mg) 4'-methyl-3-nitro-1,1'-biphenyl (**9l**). Chromatography: n-hexane/EtOAc, 8:2. ¹H-NMR (CDCl₃, 300 MHz): δ 8.53-8.54 (m, 1H), 8.32-8.35 (m, 1H), 7.98-8.02 (m, 2H), 7.22 (d, *J*= 8.3 Hz, 2H), 7.18 (d, *J*= 8.3 Hz, 2H), 2.28 (s, 3H).



Phenylboronic acid (146.4 mg, 1.2 mmol) was reacted with 1-iodo-3-nitrobenzene (249.0 mg, 1.00 mmol), K₂CO₃ (276.41 mg, 2.00 mmol) and γ-Fe₂O₃@PAMAM-G₀-Pd (7 mg, 0.47 mol%) in water at 60 °C to yield 94% (187.0 mg) 3-nitro-1,1'-biphenyl (**9m**). Chromatography: n-hexane/EtOAc, 8:2. ¹H-NMR (CDCl₃, 300 MHz): δ 8.40-8.62 (m, Ar-NO₂, 4H), 7.73-8.05 (m, 5H).

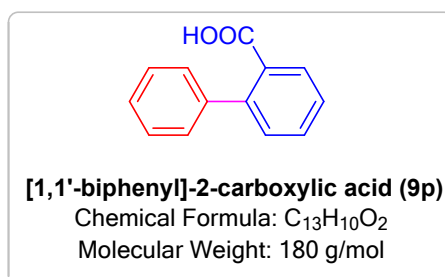


(4-nitrophenyl)boronic acid (200.0 mg, 1.2 mmol) was reacted with 1-iodo-3-nitrobenzene (249.0 mg, 1.00 mmol), K₂CO₃ (276.41 mg, 2.00 mmol) and γ-Fe₂O₃@PAMAM-G₀-Pd (7 mg, 0.47 mol%) in water at 60 °C to yield 95% (231.8 mg) 3,4'-dinitro-1,1'-biphenyl (**9n**). Chromatography: n-hexane/EtOAc, 8:2. ¹H-NMR (CDCl₃, 300 MHz): δ 7.71-8.53 (m, 8H).



Phenylboronic acid (146.4 mg, 1.2 mmol) was reacted with 1-bromo-2-methylbenzene (171.0 mg, 1.00 mmol), K₂CO₃ (276.41 mg, 2.00 mmol) and γ -Fe₂O₃@PAMAM-G₀-Pd (7 mg, 0.47 mol%) in water at 60 °C to yield 75% (139.4 mg) 2-methyl-1,1'-biphenyl (**9o**). Chromatography: n-hexane/EtOAc, 8:2. ¹H NMR (CDCl₃, 250 MHz): δ 2.26 (s, 3H), 7.28-7.48 (m, 9H).

Phenylboronic acid (146.4 mg, 1.2 mmol) was reacted with 1-chloro-2-methylbenzene (126.5 mg, 1.00 mmol), Et₃N (202.38 mg, 2.00 mmol) and γ -Fe₂O₃@PAMAM-G₀-Pd (7 mg, 0.47 mol%) in water at 90 °C to yield 60% (111.6 mg) 2-methyl-1,1'-biphenyl (product identification with GC, **9o**). Chromatography: n-hexane/EtOAc, 8:2.



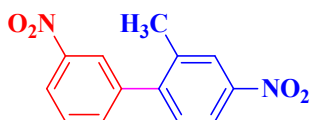
Phenylboronic acid (146.4 mg, 1.2 mmol) was reacted with 2-iodobenzoic acid (248.0 mg, 1.00 mmol), K₂CO₃ (276.41 mg, 2.00 mmol) and γ -Fe₂O₃@PAMAM-G₀-Pd (7 mg, 0.47 mol%) in water at 60 °C to yield 94% (169.2 mg) [1,1'-biphenyl]-2-carboxylic acid (**9p**). Chromatography: n-hexane/EtOAc, 8:2. ¹H-NMR (CDCl₃, 300 MHz): δ 13.65 (broad, 1H), 8.56-8.58 (m, 1H), 7.75-7.85 (m, 2H), 7.60-7.68 (m, 1H), 7.43-7.55 (m, 5H).

Phenylboronic acid (146.4 mg, 1.2 mmol) was reacted with 2-chlorobenzoic acid (156.5 mg, 1.00 mmol), Et₃N (202.38 mg, 2.00 mmol) and γ -Fe₂O₃@PAMAM-G₀-Pd (7 mg, 0.47 mol%) in water at 90 °C to yield 80% (144.0 mg) [1,1'-biphenyl]-2-carboxylic acid (product identification with GC, **9p**). Chromatography: n-hexane/EtOAc, 8:2.



2-nitro-1,1'-biphenyl (9q)
Chemical Formula: $C_{12}H_9NO_2$
Molecular Weight: 199 g/mol

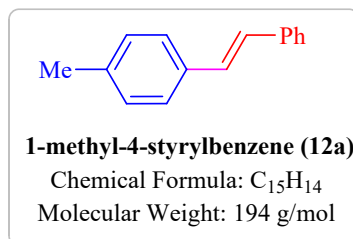
Phenylboronic acid (146.4 mg, 1.2 mmol) was reacted with 1-iodo-2-nitrobenzene (249.0 mg, 1.00 mmol), K_2CO_3 (276.41 mg, 2.00 mmol) and $\gamma\text{-Fe}_2\text{O}_3\text{@PAMAM-G}_0\text{-Pd}$ (7 mg, 0.47 mol%) in water at 60 °C to yield 80% (159.2 mg) 2-nitro-1,1'-biphenyl (**9q**). Chromatography: n-hexane/EtOAc, 8:2. $^1\text{H-NMR}$ ($CDCl_3$, 250 MHz): δ 7.43 (m, 3H), 7.58 (m, 3H), 7.9 (m, 3H).



2-methyl-3',4-dinitro-1,1'-biphenyl (9r)
Chemical Formula: $C_{13}H_{10}N_2O_4$
Molecular Weight: 258 g/mol

(3-nitrophenyl)boronic acid (200.0 mg, 1.2 mmol) was reacted with 1-iodo-2-methyl-4-nitrobenzene (263.0 mg, 1.00 mmol), K_2CO_3 (276.41 mg, 2.00 mmol) and $\gamma\text{-Fe}_2\text{O}_3\text{@PAMAM-G}_0\text{-Pd}$ (7 mg, 0.47 mol%) in water at 60 °C to yield 85% (219.2 mg) 2-methyl-3',4-dinitro-1,1'-biphenyl (**9r**). Chromatography: n-hexane/EtOAc, 8:2. $^1\text{H-NMR}$ ($CDCl_3$, 300 MHz): δ 8.13-8.33 (m, 4H), 7.31-7.75 (m, 3H), 2.42 (s, 3H).

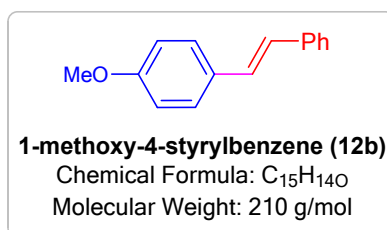
9. Data of Heck Products



Styrene (156.0 mg, 1.5 mmol) was reacted with 1-iodo-4-methylbenzene (218.0 mg, 1 mmol), K₂CO₃ (276.41 mg, 2.00 mmol) and γ -Fe₂O₃@PAMAM-G₀-Pd (8 mg, 0.67 mol%) in water at 80 °C to yield 75% (145.4 mg) 1-methyl-4-styrylbenzene (**12a**). Chromatography: n-hexane/EtOAc, 8:2. ¹H-NMR (250 MHz, CDCl₃) δ : 2.27 (s, 3H), 6.91-7.65 (m, 9H).

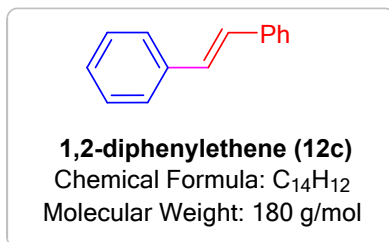
Styrene (156.0 mg, 1.5 mmol) was reacted with 1-bromo-4-methylbenzene (171.0 mg, 1 mmol), K₂CO₃ (276.41 mg, 2.00 mmol) and γ -Fe₂O₃@PAMAM-G₀-Pd (8 mg, 0.67 mol%) in water at 80 °C to yield 65% (126.0 mg) 1-methyl-4-styrylbenzene (product identification with GC, **12a**). Chromatography: n-hexane/EtOAc, 8:2.

Styrene (156.0 mg, 1.5 mmol) was reacted with 1-chloro-4-methylbenzene (126.5 mg, 1 mmol), Et₃N (202.38 mg, 2.00 mmol) and γ -Fe₂O₃@PAMAM-G₀-Pd (8 mg, 0.67 mol%) in water at 90 °C to yield 55% (106.6 mg) 1-methyl-4-styrylbenzene (product identification with GC, **12a**). Chromatography: n-hexane/EtOAc, 8:2.



Styrene (156.0 mg, 1.5 mmol) was reacted with 1-iodo-4-methoxybenzene (234.0 mg, 1 mmol), K₂CO₃ (276.41 mg, 2.00 mmol) and γ -Fe₂O₃@PAMAM-G₀-Pd (8 mg, 0.67 mol%) in water at 80 °C to yield 90% (189.0 mg) 1-methoxy-4-styrylbenzene (**12b**). Chromatography: n-hexane/EtOAc, 8:2. ¹H NMR (250 MHz, CDCl₃): δ 3.78 (s, 3H), 6.81 (d, 2H, *J* = 8.6 Hz), 6.89 (d, 1H, *J* = 16.6 Hz), 6.99 (d, 1H, *J* =

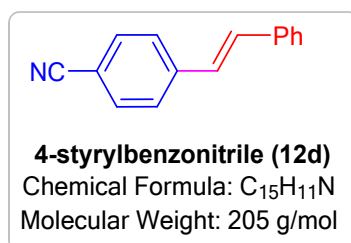
16.01 Hz), 7.19 (t, 1H, $J= 6.6$ Hz), 7.28 (t, 2H, $J= 7.6$ Hz), 7.38(d, 2H, $J= 8.6$ Hz), 7.43 (d, 2H, $J= 7.6$ Hz).



Styrene (156.0 mg, 1.5 mmol) was reacted with iodobenzene (204.0 mg, 1 mmol), K₂CO₃ (276.41 mg, 2.00 mmol) and γ -Fe₂O₃@PAMAM-G₀-Pd (8 mg, 0.67 mol%) in water at 80 °C to yield 95% (171.0 mg) 1,2-diphenylethene (**12c**). Chromatography: n-hexane/EtOAc, 8:2. ¹H-NMR (250 MHz, CDCl₃): δ 7.14 (m, 2H), 7.32 (m, 6H), 7.53 (m, 4H).

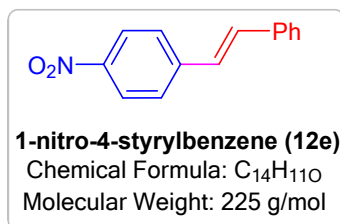
Styrene (156.0 mg, 1.5 mmol) was reacted with bromobenzene (157.0 mg, 1 mmol), K₂CO₃ (276.41 mg, 2.00 mmol) and γ -Fe₂O₃@PAMAM-G₀-Pd (8 mg, 0.67 mol%) in water at 80 °C to yield 95% (171.0 mg) 1,2-diphenylethene (product identification with GC, **12c**). Chromatography: n-hexane/EtOAc, 8:2.

Styrene (156.0 mg, 1.5 mmol) was reacted with chlorobenzene (112.5 mg, 1 mmol), Et₃N (202.38 mg, 2.00 mmol) and γ -Fe₂O₃@PAMAM-G₀-Pd (8 mg, 0.67 mol%) in water at 90 °C to yield 90% (162.0 mg) 1,2-diphenylethene (product identification with GC, **12c**). Chromatography: n-hexane/EtOAc, 8:2.



Styrene (156.0 mg, 1.5 mmol) was reacted with 4-iodobenzonitrile (229.0 mg, 1 mmol), K₂CO₃ (276.41 mg, 2.00 mmol) and γ -Fe₂O₃@PAMAM-G₀-Pd (8 mg, 0.67 mol%) in water at 80 °C to yield 85% (174.2 mg) 4-styrylbenzonitrile (**12d**). Chromatography: n-hexane/EtOAc, 8:2. ¹H NMR (250 MHz, CDCl₃):

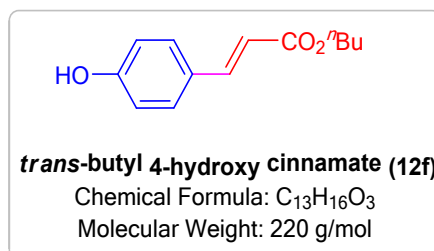
δ 7.03 (d, J = 16.6 Hz, 1H), 7.46-7.63 (m, 6H), 7.49 (t, J = 7.6 Hz, 2H), 7.42 (t, J = 7.46 Hz, 1H), 7.22 (d, J = 16.6 Hz, 1H).



Styrene (156.0 mg, 1.5 mmol) was reacted with 1-iodo-4-nitrobenzene (249.0 mg, 1 mmol), K₂CO₃ (276.41 mg, 2.00 mmol) and γ -Fe₂O₃@PAMAM-G₀-Pd (8 mg, 0.67 mol%) in water at 80 °C to yield 95% (213.6 mg) 1-nitro-4-styrylbenzene (**12e**). Chromatography: n-hexane/EtOAc, 8:2. ¹H NMR (250 MHz, CDCl₃): δ 7.24 (d, J = 16.6 Hz, 1H), 7.38 (d, J = 16.02 Hz, 1H), 7.47-7.57 (m, 3H), 7.71 (d, J = 7.4 Hz, 2H), 7.82 (d, J = 9.4 Hz, 2H), 8.41 (d, J = 9.4 Hz, 2H).

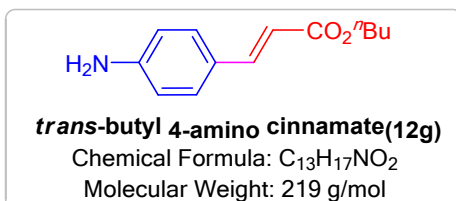
Styrene (156.0 mg, 1.5 mmol) was reacted with 1-bromo-4-nitrobenzene (202.0 mg, 1 mmol), K₂CO₃ (276.41 mg, 2.00 mmol) and γ -Fe₂O₃@PAMAM-G₀-Pd (8 mg, 0.67 mol%) in water at 80 °C to yield 95% (213.6 mg) 1-nitro-4-styrylbenzene (product identification with GC, **12e**). Chromatography: n-hexane/EtOAc, 8:2.

Styrene (156.0 mg, 1.5 mmol) was reacted with 1-chloro-4-nitrobenzene (157.5 mg, 1 mmol), Et₃N (202.38 mg, 2.00 mmol) and γ -Fe₂O₃@PAMAM-G₀-Pd (8 mg, 0.67 mol%) in water at 90 °C to yield 90% (202.4 mg) 1-nitro-4-styrylbenzene (product identification with GC, **12e**). Chromatography: n-hexane/EtOAc, 8:2.

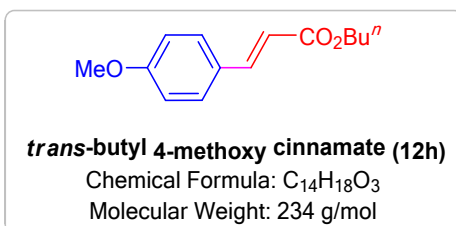


Butyl acrylate (192.2 mg, 1.5 mmol) was reacted with 4-iodophenol (220.0 mg, 1 mmol), K₂CO₃ (276.41 mg, 2.00 mmol) and γ -Fe₂O₃@PAMAM-G₀-Pd (8 mg, 0.67 mol%) in water at 80 °C to yield 90% (198.0 mg) trans-butyl 4-hydroxy cinnamate (**12f**). Chromatography: n-hexane/EtOAc, 8:2. ¹H-

NMR (250 MHz, CDCl₃): δ 0.86 (t, J = 7.6 Hz, 3H), 1.33 (m, 2H), 1.52 (m, 2H), 4.15 (t, J = 7.56 Hz, 2H), 6.21 (d, J = 12.7 Hz, 1H), 6.82 (d, J =7.6 Hz, 3H), 7.31 (d, J =10 Hz, 2H), 7.56 (d, J =15.10 Hz, 1H).

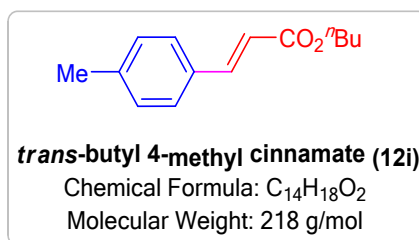


Butyl acrylate (192.2 mg, 1.5 mmol) was reacted with 4-iodoaniline (219.0 mg, 1 mmol), K₂CO₃ (276.41 mg, 2.00 mmol) and γ -Fe₂O₃@PAMAM-G₀-Pd (8 mg, 0.67 mol%) in water at 80 °C to yield 90% (197.0 mg) *trans*-butyl 4-amino cinnamate (**12g**). Chromatography: n-hexane/EtOAc, 8:2. ¹H NMR (400MHz, CDCl₃, TMS): δ 7.58 (d, J = 16.0 Hz, 1H), 7.36 (d, J = 8.5 Hz, 2H), 6.68 (d, J = 8.0 Hz, 2H), 4.32 (s, 2H, NH₂), 6.25 (d, J = 16.0 Hz, 1H), 4.17 (t, J = 6.9 Hz, 2H), 1.72-1.65 (m, 2H), 1.44 (sext, J = 7.3 Hz, 2H), 0.95 (t, J = 7.3 Hz, 3H).



Butyl acrylate (192.2 mg, 1.5 mmol) was reacted with 1-iodo-4-methoxybenzene (234.0 mg, 1 mmol), K₂CO₃ (276.41 mg, 2.00 mmol) and γ -Fe₂O₃@PAMAM-G₀-Pd (8 mg, 0.67 mol%) in water at 80 °C to yield 92% (215.2 mg) *trans*-butyl 4-methoxy cinnamate (**12h**). Chromatography: n-hexane/EtOAc, 8:2. ¹H NMR (250 MHz, CDCl₃): δ 0.88 (t, J = 7.6 Hz, 3H), 1.34 (m, 2H), 1.62 (quint, 2H, J = 5.0 Hz), 3.77 (s, 3H), 4.12 (t, 2H, J = 6.8 Hz), 6.24 (d, J = 16.0 Hz, 1H), 6.83 (d, J = 5.0 Hz, 2H), 7.42 (d, J = 5.0 Hz, 2H), 7.56 (d, J = 16.0 Hz, 1H).

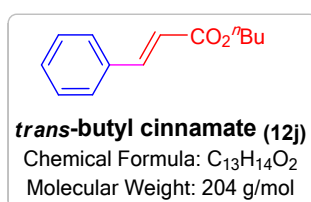
Butyl acrylate (192.2 mg, 1.5 mmol) was reacted with 1-chloro-4-methoxybenzene (142.5 mg, 1 mmol), Et₃N (152.0 mg, 2.00 mmol) and γ -Fe₂O₃@PAMAM-G₀-Pd (8 mg, 0.67 mol%) in water at 90 °C to yield 65% (152.0 mg) *trans*-butyl 4-methoxy cinnamate (product identification with GC, **12h**). Chromatography: n-hexane/EtOAc, 8:2.



Butyl acrylate (192.2 mg, 1.5 mmol) was reacted with 1-iodo-4-methylbenzene (218.0 mg, 1 mmol), K₂CO₃ (276.41 mg, 2.00 mmol) and γ -Fe₂O₃@PAMAM-G₀-Pd (8 mg, 0.67 mol%) in water at 80 °C to yield 80% (174.4 mg) *trans*-butyl 4-methyl cinnamate (**12i**). Chromatography: n-hexane/EtOAc, 8:2. ¹H-NMR (250 MHz, CDCl₃): δ 0.84 (t, *J* = 4.8 Hz, 3H), 1.31 (m, 2H), 1.54 (m, 2H), 2.25 (s, 3H), 4.11 (t, *J* = 5.0 Hz, 2H), 6.31 (dd, *J* = 16.0 Hz, *J'* = 5.10 Hz, 1H), 7.05 (m, 2H), 7.29 (m, 2H), 7.51 (dd, *J* = 18.3 Hz, *J'* = 5.6 Hz, 1H).

Butyl acrylate (192.2 mg, 1.5 mmol) was reacted with 1-bromo-4-methylbenzene (171.0 mg, 1 mmol), K₂CO₃ (276.41 mg, 2.00 mmol) and γ -Fe₂O₃@PAMAM-G₀-Pd (8 mg, 0.67 mol%) in water at 80 °C to yield 80% (174.4 mg) *trans*-butyl 4-methyl cinnamate (product identification with GC, **12i**). Chromatography: n-hexane/EtOAc, 8:2.

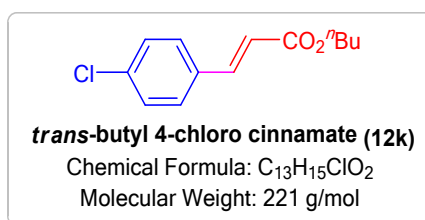
Butyl acrylate (192.2 mg, 1.5 mmol) was reacted with 1-chloro-4-methylbenzene (126.5 mg, 1 mmol), Et₃N (202.38 mg, 2.00 mmol) and γ -Fe₂O₃@PAMAM-G₀-Pd (8 mg, 0.67 mol%) in water at 90 °C to yield 70% (152.6 mg) *trans*-butyl 4-methyl cinnamate (product identification with GC, **12i**). Chromatography: n-hexane/EtOAc, 8:2.



Butyl acrylate (192.2 mg, 1.5 mmol) was reacted with iodobenzene (204.0 mg, 1 mmol), K₂CO₃ (276.41 mg, 2.00 mmol) and γ -Fe₂O₃@PAMAM-G₀-Pd (8 mg, 0.67 mol%) in water at 80 °C to yield 95% (193.2 mg) *trans*-butyl cinnamate (**12j**). Chromatography: n-hexane/EtOAc, 8:2. ¹H-NMR (250 MHz, CDCl₃): δ 0.92 (t, *J* = 7.5 Hz, 3H), 1.39 (m, 2H), 1.65 (m, 2H), 4.17 (t, *J* = 6.8 Hz, 2H), 6.54 (d, *J* = 16.0 Hz, 1H), 7.63 (d, *J* = 8.8 Hz, 2H), 7.65 (d, *J* = 16.3 Hz, 1H), 8.19 (d, *J* = 8.8 Hz, 2H).

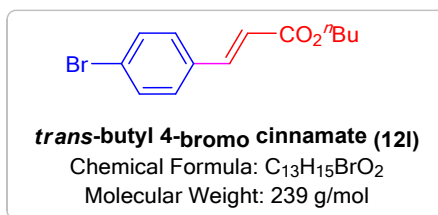
Butyl acrylate (192.2 mg, 1.5 mmol) was reacted with bromobenzene (157.0 mg, 1 mmol), K_2CO_3 (276.41 mg, 2.00 mmol) and $\gamma\text{-Fe}_2\text{O}_3\text{@PAMAM-G}_0\text{-Pd}$ (8 mg, 0.67 mol%) in water at 80 °C to yield 90% (183.6 mg) *trans*-butyl cinnamate (product identification with GC, **12j**). Chromatography: n-hexane/EtOAc, 8:2.

Butyl acrylate (192.2 mg, 1.5 mmol) was reacted with chlorobenzene (112.5 mg, 1 mmol), Et_3N (202.38 mg, 2.00 mmol) and $\gamma\text{-Fe}_2\text{O}_3\text{@PAMAM-G}_0\text{-Pd}$ (8 mg, 0.67 mol%) in water at 90 °C to yield 80% (163.2 mg) *trans*-butyl cinnamate (product identification with GC, **12j**). Chromatography: n-hexane/EtOAc, 8:2.

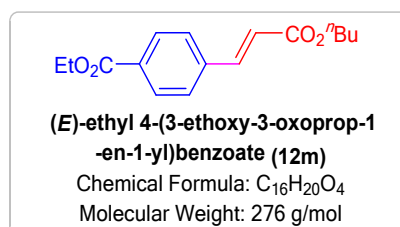


Butyl acrylate (192.2 mg, 1.5 mmol) was reacted with 1-chloro-4-iodobenzene (238.4 mg, 1 mmol), K_2CO_3 (93.9 mg, 2.00 mmol) and $\gamma\text{-Fe}_2\text{O}_3\text{@PAMAM-G}_0\text{-Pd}$ (8 mg, 0.67 mol%) in water at 80 °C to yield 85% (187.8 mg) *trans*-butyl 4-chloro cinnamate (**12k**). Chromatography: n-hexane/EtOAc, 8:2. 1H NMR (400Hz, $CDCl_3$, TMS): δ 7.65 (d, $J = 16.0$ Hz, 1H), 7.49 (dd, $J = 6.9, 2.0$ Hz, 2H), 6.92-6.87 (m, 2H), 6.32 (d, $J = 15.7$ Hz, 1H), 4.19 (t, $J = 6.9$ Hz, 1H), 4.13 (t, $J = 4.5$ Hz, 1H), 1.69 (dd, $J = 14.9, 7.0$ Hz, 2H), 1.47-1.42 (m, 2H), 0.99-0.92 (m, 3H).

Butyl acrylate (192.2 mg, 1.5 mmol) was reacted with 1-bromo-4-chlorobenzene (191.4 mg, 1 mmol), Et_3N (202.38 mg, 2.00 mmol) and $\gamma\text{-Fe}_2\text{O}_3\text{@PAMAM-G}_0\text{-Pd}$ (8 mg, 0.67 mol%) in water at 90 °C to yield 70% (154.6 mg) *trans*-butyl 4-chloro cinnamate (product identification with GC, **12k**). Chromatography: n-hexane/EtOAc, 8:2.



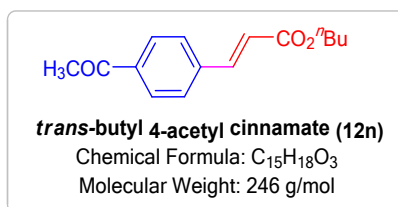
Butyl acrylate (192.2 mg, 1.5 mmol) was reacted with 1-bromo-4-iodobenzene (282.9 mg, 1 mmol), K₂CO₃ (93.9 mg, 2.00 mmol) and γ -Fe₂O₃@PAMAM-G₀-Pd (8 mg, 0.67 mol%) in water at 80 °C to yield 75% (179.2 mg) *trans*-butyl 4-bromo cinnamate (**12l**). Chromatography: n-hexane/EtOAc, 8:2. ¹H-NMR (250 MHz, CDCl₃): δ 0.89 (t, 3H, *J* = 7.7 Hz), 1.36 (m, 2H), 1.64 (m, 2H), 4.14 (t, 2H, *J* = 7.7 Hz), 6.36 (d, 1H, *J* = 17.7 Hz), 7.21-7.32 (m, 2H), 7.42-7.44 (m, 2H), 7.53 (d, 1H, *J* = 17.57 Hz).



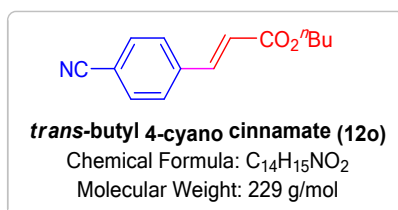
Butyl acrylate (192.2 mg, 1.5 mmol) was reacted with ethyl 4-iodobenzoate (165.1 mg, 1 mmol), K₂CO₃ (93.9 mg, 2.00 mmol) and γ -Fe₂O₃@PAMAM-G₀-Pd (8 mg, 0.67 mol%) in water at 80 °C to yield 95% (262.2 mg) (E)-ethyl 4-(3-ethoxy-3-oxoprop-1-en-1-yl)benzoate (**12m**). Chromatography: n-hexane/EtOAc, 8:2. ¹H NMR (400Hz, CDCl₃, TMS): δ 8.06 (dd, *J* = 6.9, 1.6 Hz, 2H), 7.68 (d, *J* = 16.0 Hz, 1H), 7.59 (d, *J* = 8.5 Hz, 2H), 6.53 (d, *J* = 16.0 Hz, 1H), 4.38 (dd, *J* = 14.0, 7.3 Hz, 2H), 4.22 (t, *J* = 8.3 Hz, 2H), 1.76-1.65 (m, 2H), 1.48-1.33 (m, 5H), 0.97 (t, *J* = 7.3 Hz, 3H).

Butyl acrylate (192.2 mg, 1.5 mmol) was reacted with ethyl 4-bromobenzoate (229.0 mg, 1 mmol), K₂CO₃ (276.41 mg, 2.00 mmol) and γ -Fe₂O₃@PAMAM-G₀-Pd (8 mg, 0.67 mol%) in water at 80 °C to yield 93% (256.6 mg) (E)-ethyl 4-(3-ethoxy-3-oxoprop-1-en-1-yl)benzoate (product identification with GC, **12m**). Chromatography: n-hexane/EtOAc, 8:2.

Butyl acrylate (192.2 mg, 1.5 mmol) was reacted with ethyl 4-chlorobenzoate (156.5 mg, 1 mmol), Et₃N (202.38 mg, 2.00 mmol) and γ -Fe₂O₃@PAMAM-G₀-Pd (8 mg, 0.67 mol%) in water at 90 °C to yield 90% (248.4 mg) (E)-ethyl 4-(3-ethoxy-3-oxoprop-1-en-1-yl)benzoate (product identification with GC, **12m**). Chromatography: n-hexane/EtOAc, 8:2.

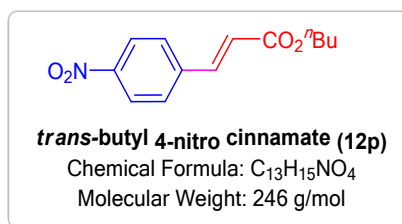


Butyl acrylate (192.2 mg, 1.5 mmol) was reacted with 1-(4-iodophenyl)ethanone (246.0 mg, 1 mmol), K₂CO₃ (93.9 mg, 2.00 mmol) and γ -Fe₂O₃@PAMAM-G₀-Pd (8 mg, 0.67 mol%) in water at 80 °C to yield 90% (221.4 mg) *trans*-butyl 4-acetyl cinnamate (**12n**). Chromatography: n-hexane/EtOAc, 8:2. ¹H NMR (400Hz, CDCl₃, TMS): δ 8.00 (d, J = 8.5 Hz, 1H), 7.98 (d, J = 8.5 Hz, 1H), 7.68 (dd, J = 16.5, 1.6 Hz, 1H), 7.61 (dd, J = 8.5, 2.3 Hz, 2H), 6.55 (dd, J = 16.0, 1.3 Hz, 1H), 4.23 (t, J = 6.7 Hz, 2H), 4.05 (t, J = 6.7 Hz, 2H), 2.63 (s, 3H), 0.98 (t, J = 7.5 Hz, 3H), 0.92 (t, J = 7.7 Hz, 3H).

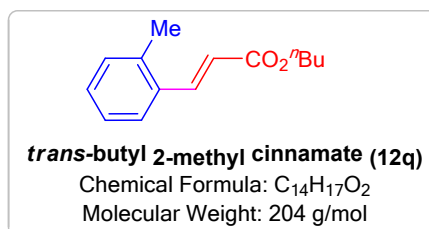


Butyl acrylate (192.2 mg, 1.5 mmol) was reacted with 4-bromobenzonitrile (182.0 mg, 1 mmol), K₂CO₃ (93.9 mg, 2.00 mmol) and γ -Fe₂O₃@PAMAM-G₀-Pd (8 mg, 0.67 mol%) in water at 80 °C to yield 92% (210.6 mg) *trans*-butyl 4-cyano cinnamate (**12o**). Chromatography: n-hexane/EtOAc, 8:2. ¹H-NMR (250 MHz, CDCl₃): δ 0.89 (t, J = 7.3 Hz, 3H), 1.36 (m, 2H), 1.65 (m, 2H), 4.17 (t, J = 6.6 Hz, 2H), 6.49 (d, J = 16 Hz, 1H), 7.60, (m, 5H).

Butyl acrylate (192.2 mg, 1.5 mmol) was reacted with 4-chlorobenzonitrile (137.5 mg, 1 mmol), Et₃N (202.38 mg, 2.00 mmol) and γ -Fe₂O₃@PAMAM-G₀-Pd (8 mg, 0.67 mol%) in water at 90 °C to yield 85% (194.6 mg) *trans*-butyl 4-cyano cinnamate (product identification with GC, **12o**). Chromatography: n-hexane/EtOAc, 8:2.

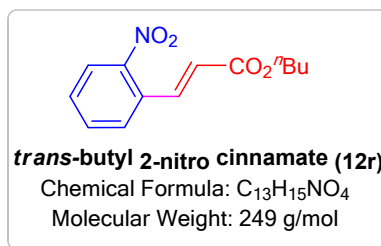


Butyl acrylate (192.2 mg, 1.5 mmol) was reacted with 1-iodo-4-chlorobenzene (238.4 mg, 1 mmol), K₂CO₃ (93.9 mg, 2.00 mmol) and γ -Fe₂O₃@PAMAM-G₀-Pd (8 mg, 0.67 mol%) in water at 80 °C to yield 95% (233.6 mg) *trans*-butyl 4-nitro cinnamate (**12p**). Chromatography: n-hexane/EtOAc, 8:2. ¹H-NMR (250 MHz, CDCl₃): δ 0.98 (t, *J* = 7.3 Hz, 3H), 1.46 (m, 2H), 1.68 (m, 2H), 4.24 (t, *J* = 7.6 Hz, 2H), 6.55 (dd, *J* = 16.0 Hz, *J'* = 6.3 Hz, 1H), 7.68 (m, 3H), 8.25 (m, 2H).



Butyl acrylate (192.2 mg, 1.5 mmol) was reacted with 1-bromo-2-methylbenzene (171.0 mg, 1 mmol), K₂CO₃ (93.9 mg, 2.00 mmol) and γ -Fe₂O₃@PAMAM-G₀-Pd (8 mg, 0.67 mol%) in water at 80 °C to yield 92% (187.6 mg) *trans*-butyl 2-methyl cinnamate (**12q**). Chromatography: n-hexane/EtOAc, 8:2. ¹H-NMR (250 MHz, CDCl₃): δ 0.86 (t, *J* = 2.6 Hz, 3H), 1.33 (m, 2H), 1.58 (m, 2H), 2.31 (s, 3H), 4.12 (t, 2H), 6.28 (dd, *J* = 15.9 Hz, *J'* = 4.9 Hz, 1H), 7.12 (m, 3H), 7.42 (m, 1H), 7.85 (dd, *J* = 13.8 Hz, *J'* = 4.2 Hz, 1H).

Butyl acrylate (192.2 mg, 1.5 mmol) was reacted with 1-chloro-2-methylbenzene (126.5 mg, 1 mmol), Et₃N (202.38 mg, 2.00 mmol) and γ -Fe₂O₃@PAMAM-G₀-Pd (8 mg, 0.67 mol%) in water at 90 °C to yield 50% (102.0 mg) *trans*-butyl 2-methyl cinnamate (product identification with GC, **12q**). Chromatography: n-hexane/EtOAc, 8:2.



Butyl acrylate (192.2 mg, 1.5 mmol) was reacted with 1-iodo-4-chlorobenzene (238.4 mg, 1 mmol), K₂CO₃ (93.9 mg, 2.00 mmol) and γ -Fe₂O₃@PAMAM-G₀-Pd (8 mg, 0.67 mol%) in water at 80 °C to yield 92% (229.0 mg) *trans*-butyl 2-nitro cinnamate (**12r**). Chromatography: n-hexane/EtOAc, 8:2. ¹H-NMR (250 MHz, CDCl₃): δ 0.89 (t, *J*= 7.6 Hz, 3H), 1.36 (m, 2H), 1.63 (m, 2H), 4.15 (t, *J*= 7.6 Hz, 2H), 6.28 (d, *J*= 17.6 Hz, 1H), 7.43-7.58 (m, 2H), 7.95-7.98 (m, 2H), 8.03 (d, *J*= 17.6 Hz, 1H).

10. References

- (1) Sobhani, S. and Z. Pakdin-Parizi, *Appl. Catal. A Gen.* 2014, **479**, 112.
- (2) Beezer, A. E. King, A. S. H. Martin, I. K. Mitchel, J. C.; Twyman, L. J. and C. F. Wain, *Tetrahedron* 2003, **59**, 3873.
- (3) Zolfigol, M. A. Ayazi-Nasrabadi, R. and S. Bagheri, *Appl. Organomet. Chem.* 2016, **30**, 500.
- (4) Huang, J. Su, P. Zhou, L. and Y. Yang, *Colloids Surfaces A Physicochem. Eng. Asp.* 2016, **490**, 241.
- (5) Yilmaz Baran, N. Baran, T. and A. Menteş, *Appl. Clay Sci.* 2019, **181**, 105225.
- (6) Alinezhad, H. Amiri, A. Tarahomi, M. and B. Maleki, *Talanta* 2018, **183**, 149.
- (7) Manna, A. Imae, T. Aoi, K. Okada, M. and T. Yogo, *Chem. Mater.* 2001, **13**, 1674.
- (8) Sohail, I. Bhatti, I. A. Ashar, A. Sarim, F. M. Mohsin, M. Naveed, R. Yasir, M. Iqbal, M. and A. Nazir, *J. Mater. Res. Technol.* 2020, **9**, 498.
- (9) White, B. R. Stackhouse, B. T. and J. A. Holcombe, *J. Hazard. Mater.* 2009, **161**, 848.
- (10) Hu, J. Lo, I. M. C. and G. Chen, *Sep. Purif. Technol.* 2007, **58**, 76.
- (11) Sardarian, A. R. Eslahi, H. and M. Esmailpour, *Catalyst. Appl. Organomet. Chem.* 2019, **33**, e4856.
- (12) Mohammadinezhad, A. and B. Akhlaghinia, *Green Chem.* 2017, **19**, 5625.
- (13) Sardarian, A. R. Kazemnejadi, M. and M. Esmailpour, *Dalt. Trans.* 2019, **48**, 3132.
- (14) Jiang, Y. Jiang, J. Gao, Q. Ruan, M. Yu, H. and L. Qi, *Nanotechnology.* 2008, **19**, 075714.
- (15) Murugan, E. and J. N. Jebaranjitham, *Chem. Eng. J.* 2015, **259**, 266.
- (16) Zheng, P. Gao, L. Sun, X. Mei, S. *The Thermolysis Behaviours of the First Generation Dendritic Polyamidoamine*; 2009; Vol. 18.
- (17) Ulaszewska, M. M. Hernando, M. D. Moreno, A. U. García, A. V. Calvo, E. G. and A. R.

- Fernández-Alba, *Rapid Commun. Mass Spectrom.* 2013, **27**, 747.
- (18) Darezereshki, E. *Mater. Lett.* 2010, **64**, 1471.
- (19) Sreeja, V. and P. A. Joy, *Mater. Res. Bull.* 2007, **42**, 1570.
- (20) Cui, J. Zhu, N. Kang, N. Ha, C. Shi, C. and P. Wu, *Chem. Eng. J.* 2017, **328**, 1051.
- (21) Cheng, K. Cao, D. Yang, F. Zhang, L. Xu, Y. and G. Wang, *J. Mater. Chem.* 2012, **22**, 850.
- (22) Chen, T. Gao, J. and M. Shi, *Tetrahedron* 2006, **62**, 6289.
- (23) Sabounchei, S. J. and A. Hashemi, *Inorg. Chem. Commun.* 2014, **47**, 123.
- (24) Nasrollahzadeh, M. Azarian, A. Maham, M. and A. Ehsani, *J. Ind. Eng. Chem.* 2015, **21**, 746.
- (25) Modak, A. Mondal, J. Sasidharan, M. and A. Bhaumik, *Green Chem.* 2011, **13**, 1317.
- (26) Fortea-Pérez, F. R. Schlegel, I. Julve, M. Armentano, D. De Munno, G. and S. E. Stiriba, *J. Organomet. Chem.* 2013, **743**, 102.
- (27) Singh, A. S. Patil, U. B. and J. M. Nagarkar, *Catal. Commun.* 2013, **35**, 11.
- (28) Jang, Y. Chung, J. Kim, S. Jun, S. W. Kim, B. H. Lee, D. W. Kim, B. M. and T. Hyeon, *Phys. Chem. Chem. Phys.* 2011, **13**, 2512.
- (29) Shylesh, S. Wang, L. Demeshko, S. and W. R. Thiel, *Chem. Cat. Chem.* 2010, **2**, 1543.
- (30) Yang, J. Wang, D. Liu, W. Zhang, X. Bian, F. and W. Yu, *Green Chem.* 2013, **15**, 3429.
- (31) Fortea-Pérez, F. R. Julve, M. Dikarev, E. V. Filatov, A. S. and S. E. Stiriba, *Inorganica Chim. Acta*, 2018, **471**, 788.
- (32) Li, P. Wang, L. Zhang, L. and G. W. Wang, *Adv. Synth. Catal.* 2012, **354**, 1307.
- (33) Wang, P. Liu, H. Liu, M. Li, R. and J. Ma, *New J. Chem.* 2014, **38**, 1138.
- (34) Nasrollahzadeh, M. Azarian, A. Ehsani, A. and M. Khalaj, *J. Mol. Catal. A Chem.* 2014, **394**, 205.
- (35) Erathodiyil, N. Ooi, S. Seayad, A. M. Han, Y. Lee, S. S. and J. Y. Ying, *Chem. - A Eur. J.* 2008, **14**, 3118.
- (36) Tamami, B. Farjadian, F. Ghasemi, S. and H. Allahyari, *New J. Chem.* 2013, **37**, 2011.
- (37) Kazemnejadi, M. Rezazadeh, Z. Nasser, M.A. Allahresani, A. and M. Esmailpour, *Green Chem.* 2019, **21**, 1718.
- (38) Wang, K. Liu, J. Zhang, F. Zhang, Q. Jiang, H. Tong, M. and F. Zhang, *ACS Appl. Mater. Interfa.* 2019, **11**, 41238.
- (39) Aghahosseini, H. Saadati, M.R. Rezaei, S.J.T. Ramazani, A. Asadi, N. Yahiro, H., and A. R. Kazemizadeh. *Sci. Rep.* 2021, **11**, 1.